Advances in the Design of Genuine Human Tyrosinase Inhibitors for Targeting Melanogenesis and Related Pigmentations

Brayan Roulier, Basile Pérès, and Romain Haudecoeur*

Cite This: *J. Med. Chem.* 2020, 63, 13428−13443

Read Online

ACCESS | Metrics & More | Article Recommendations

ABSTRACT: Human tyrosinase (*hs*TYR) is the key enzyme ensuring the conversion of L-tyrosine to dopaquinone, thereby initiating melanin synthesis, i.e., melanogenesis. Although the protein has long been familiar, knowledge about its three-dimensional structure and efficient overexpression protocols emerged only recently. Consequently, for decades medicinal chemistry studies aiming at developing skin depigmenting agents relied almost exclusively on biological assays performed using mushroom tyrosinase (*ab*TYR), producing a plethoric literature, often of little useful purpose. Indeed, several recent reports have pointed out spectacular differences in terms of interaction patterns and inhibition values between *hs*TYR and *ab*TYR, including for widely used standard tyrosinase inhibitors. In this review, we summarize the last developments regarding the potential role of *hs*TYR in human pathologies, the advances in recombinant expression systems and structural data retrieving, and the pioneer generation of true *hs*TYR inhibitors. Finally, we present suggestions for the design of future inhibitors of this highly attractive target in pharmacology and dermocosmetics.
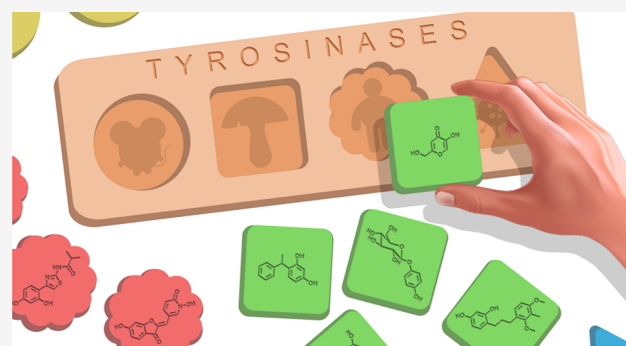
INTRODUCTION

Human tyrosinase (*hs*TYR) is a type-3 copper-containing metalloenzyme belonging to the tyrosinase (TYR, EC 1.14.18.1) family, which also includes plant, fungal, bacterial, and mammal enzymes. This glycoprotein is made of 529 amino acids, including an 18-residues N-terminal signal sequence and six or seven N-glycosylated positions, for a molecular weight of ∼67 kDa. Its active site is composed of two close, magnetically coupled copper centers, bridged by an aquo(hydroxo) ligand in the *met* state (the reactive state of *hs*TYR) and coordinated by six histidine residues (H180, H202, H211 for Cu_A, H363, H367, H390 for Cu_B), highly conserved among tyrosinases, catechol oxidases, and hemocyanins.[1] The physiological function of *hs*TYR is to carry out the *o*-hydroxylation of L-tyrosine to L-DOPA (monophenolase activity) and the subsequent oxidation of L-DOPA in dopaquinone (diphenolase activity) by using molecular oxygen, although the enzyme is able to oxidize a broad landscape of monophenolic and diphenolic substrates.[2] This double oxidation process initiates the synthesis of melanin pigments, which proceeds mostly nonenzymatically afterward. Only two other enzymes are known to be involved in melanogenesis, tyrosinase-related proteins 1 and 2 (*hs*TYRP1 and *hs*TYRP2), which display a high level of homology with *hs*TYR, although the role of *hs*TYRP1 is still unclear and could rather be linked to *hs*TYR protection.[3] The ultimate products of this process called melanogenesis are eumelanin and pheomelanin, depending on the absence or the presence of nucleophilic

cysteines. Eumelanin is mostly a dark brown to black polymer of 5,6-dihydroxyindole and 5,6-dihydroxyindole-2-carboxylic acid units, with some indole rings cleaved into pyrrole counterparts. Pheomelanin, a yellow to red polymer, is made of benzothiazine and benzothiazole units (Figure 1).[4] Overall, melanogenesis occurs in specialized dendritic cells called melanocytes, located in human skin, hair bulb, and eyes. At the subcellular level, the production of melanins is confined in melanosomes, unique membrane-bound organelles, as the process is otherwise susceptible to provide chemical hazard and genomic instability to melanocytes. Melanins are essential epidermis components that ensure crucial skin protection against UV radiation and free radicals, but abnormal levels of the pigment are linked to several pathologies. The role of *hs*TYR in the melanogenic process is central, as the enzyme catalyzes the rate-limiting first two steps of the reaction sequence (Figure 1). Thus, most of the efforts aiming to suppress or reduce melanogenesis *in vivo* have been dedicated to the search of TYR inhibitors. The strategy has proven to be effective, and clear correlations have been observed
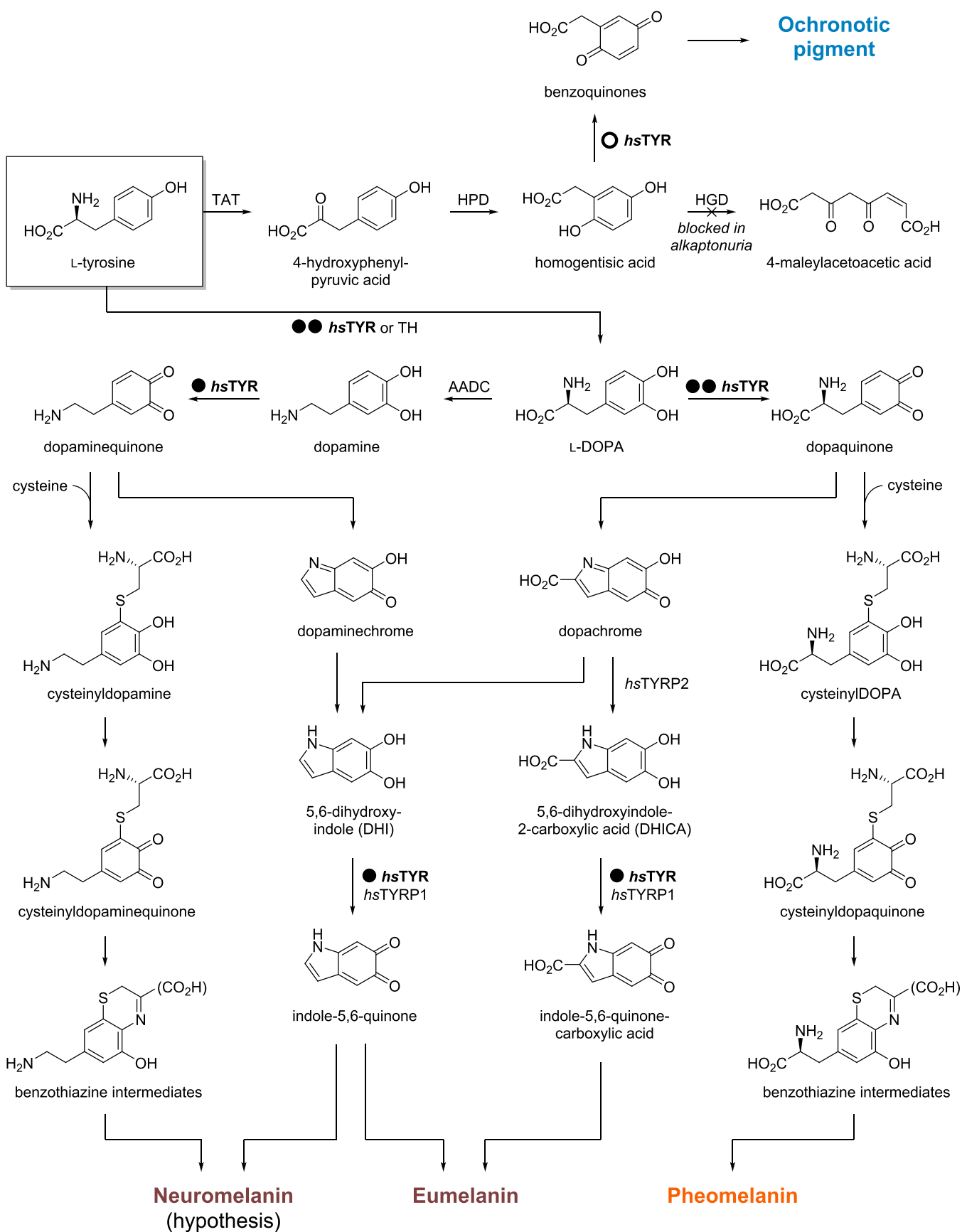
Figure 1. L-Tyrosine-related pigmentation biochemical pathways involving *hs*TYR as a demonstrated (●●), suspected (●) or purely hypothetic (○) component.

between the inhibition of TYR and the level of pigmentation produced. Therefore, *hs*TYR appears as a convenient and attractive target for reducing human melanogenesis in various contexts. However, many obstacles have long littered the path to efficient *hs*TYR inhibitor design, sparking exciting scientific breakthroughs that were achieved only very recently.

In this review, we will provide an overview of current hypotheses of the involvement of *hs*TYR in pathologies, such as hyperpigmentations, melanoma, Parkinson's disease, or alkaptonuria. Limitations, challenges, and innovations in drug design strategies for developing *hs*TYR inhibitors will be discussed, as the field has undergone a significant evolution in the past few years. Forerunning genuine *hs*TYR inhibitors will be presented with an emphasis on clinical data reported, and observations and suggestions will be drawn as a guidance for future *hs*TYR-targeting drug design stories.

■ HUMAN TYROSINASE AS A SUITABLE THERAPEUTIC TARGET

Dermatological and Cosmetic Applications of Skin-Whitening Agents. Skin whitening appears as the most obvious and sought application for *hs*TYR inhibitors. This practice, common in some ethnic groups, especially in Asia, Africa, and the Middle East, is the result of a complex interplay of cultural, social, political, and psychological factors and is documented since the dawn of human civilizations, e.g., the quest of "skin like white jade" in the first Korean Dynasty (Gojoseon era, 2333−108 B.C.).[5] Lighter skin complexion is often associated with beauty and health in these cultures, while darker skin tones are pejoratively linked to lower social conditions, and thus since the 1980s the interest in skin whitening has exponentially grown.[6] As a consequence, about 28% of the global population practices skin-whitening at least once in a lifetime,[7] and it is estimated that the worldwide market associated with these cosmetics could reach 23 billion dollars by 2020;[8] it is worth noting that, quite paradoxically, the use of skin-darkening agents is also a multibillion dollars market, including the use of illegal tanning drugs increasing melanogenesis, such as melanotan II.[9] Besides, depigmentation is also a medical need for patients suffering from common to very rare dermatological disorders related to hyperpigmentation. In particular, melasma, solar lentigo, erythromelanosis follicularis faciei et colli, erythema dyschromicum perstans, congenital melanocytic naevi, or postinflammatory hyperpigmentation can cause health issues and disfigurements, sometimes severe and affecting facial aesthetics, with a high negative impact on a patient's psychology and quality of life.[10] Among the existing skin-whitening agents widely used for both cosmetic and dermatological purposes, hydroquinone, kojic acid, arbutin, azelaic acid, ellagic acid, and resveratrol are the most common. However, all of these agents lack efficacy and/or safety (*vide infra*). Hydroquinone, the gold standard used for decades, frequently induces skin irritation and, upon chronic exposure, exogenous ochronosis, allergic contact dermatitis, conjunctival melanosis, nail discoloration, and corneal degeneration. In addition, it was associated with bone-marrow toxicity, immunotoxicity, nephrotoxicity, mutagenicity, and carcinogenesis, especially through the formation of 1,4-benzoquinone by oxidation (either spontaneously in the presence of oxygen or upon enzymatic activity) that results in the production of polymers and toxic mono- and polyglutathione conjugates.[11] Thus, hydroquinone was banned by EU Cosmetic Regulation.[12] Kojic acid also triggers carcinogenicity and instability issues, and

its use has been restricted to 1% in cosmetic preparations in the EU, while other compounds such as ellagic acid appear as not suitable for clinical use.[13] Overall, there is a great need for nontoxic skin-whitening agents for meeting the social needs in terms of safe cosmetic practices and medical hyperpigmentation treatments, and *hs*TYR appears as a target of choice.

Benefit of Antimelanogenic Adjuvants for Melanoma Therapies. It was shown recently that *hs*TYR inhibition could also bring benefits in the frame of melanoma management.[14] Melanoma is the deadliest form of skin cancer, accounting for about 1% of skin cancer cases but more than 60% of related deaths (data from the U.S.).[15] Worldwide, melanoma causes a total of ∼55 000 deaths annually.[16] The high lethality rate of melanoma is due to multiple resistance to current anticancer therapy, especially in late stages III and IV of the disease. With standard dacarbazine chemotherapy, the median overall survival is 6−10 months at stage IV, with a 5-year survival rate of ∼10%, a value recently extended to ∼20% using innovative immunotherapy approaches involving specific immune-checkpoints targeting.[17] Indeed, unlike normal human melanocytes, melanoma cells do not transfer their melanin production to adjacent keratinocytes, accumulating the pigment instead. The resulting high concentration of intracellular melanin, proportionally related to a shortening of overall survival in patients,[18] induces several harmful consequences. First, melanin has been long recognized for conferring radioprotective effects to melanoma cells, even if radiotherapy, initially dismissed as ineffective, is now seen as beneficial in some cases.[19] Recently, a clear relation between the attenuated efficacy of radiotherapy and the level of melanin accumulation has been unraveled, suggesting that inhibiting melanogenesis could sensitize melanoma cells and improve the global outcome.[20] Indeed, the treatment of melanoma cells with phenylthiourea as an *hs*TYR inhibitor (K_i = 1.7 μM)[2] *in vitro* actually led to an increased susceptibility of cells to γ rays, providing support for future *in vivo* experiments.[21] Furthermore, melanin can chelate and neutralize chemotherapeutic agents. Indeed, the response to cyclophosphamide treatment was found higher in nonpigmented melanoma cells than in pigmented counterparts, and the whitening action of phenylthiourea on pigmented cells clearly sensitized them to the chemotherapeutic action (significant cell killing upon micromolar cyclophosphamide treatment in the presence of phenylthiourea vs millimolar treatment for control).[22] The broad absorption spectrum of melanin also causes interferences with the light used for irradiation in photodynamic therapy (PDT). Transmittance in melanotic melanoma only occurs beyond 700 nm, dismissing a large number of classical photosensitizers, such as hypericin or photofrin.[23] Furthermore, the scavenging properties of melanin protect melanoma cells from PDT-induced reactive oxygen species (ROS), including singlet oxygen.[24] The suppression of melanogenesis increased the susceptibility of melanoma cells to hypericin-mediated PDT and caused a rise of ROS level, using both phenylthiourea and kojic acid (K_i = 350 μM)[2] as *hs*TYR inhibitors.[25,26] Lastly, intermediates of melanogenesis such as L-DOPA and reactive quinones are known to be immunosuppressive and/or selectively lymphotoxic.[27] While pigmented melanoma cells were resistant to peripheral blood lymphocyte-mediated cytotoxicity despite the presence of melanoma-associated antigens, the same cells depigmented in the presence of phenylthiourea showed a strikingly enhanced susceptibility (∼50% of melanoma cells killed with 1 mM phenylthiourea vs <0.1% for control)[22] that could endorse the development of

```
hsTYR    172   IYDLFVWMHYYVSMDALLG-GSEIWRDIDFAHEAPAFLPWHRLFLLRWEQEIQKLTGDENFTIPYWDWRDAEK------C
hsTYRP1  184   IYNYFVWTHYYSVKKTFLGVGQESFGEVDFSHEGPAFLTWHRYHLLRLEKDMQEMLQEPSFSLPYWNFATGKNV-----C
scTYR     30   RYDEFVRTHNEFIMSDTD--------GERTGHRSPSFLPWHRRFLLDFEQALQSVD--SSVTLPYWDWSADR-----TVR
abPPO3    53    SFFQLGGIHGL-----------LHLYKANYCTHGTVLFPTWHRAYESTWEQTLWEAAGAKDLRQPFWDWGYW-DFIGLPD-
abPPO4    49    SFFQLSGIHGL------------PYESGYCTHSQVLFPTWHRVYVSIYEQILQEAAKAEDLRQPYWDTGFAL---VPPD-
                :    :     *                      *     *  .***  .     *:  :  .        ..  *:*.:*:
```

```
hsTYR    245   DICTDEYMGGQHPTPNLLSPASFFSSWQIVCSRLEEYNSHQSLCNGTPEGPLRRN-PGNHDKSRTPRLPSSADVEFCLS
hsTYRP1  259   DICTDDLMGSRSNFDSTLISPNSVFSQWRVVCDSLEDYDTLGTLCNSTEDGPIRRNPAGNVARPMVQRLPEPQDVAQCLE
scTYR     96   ALWAPDFLGGTGRSTDGRVMD-GPFAAWPINVRVD-------------RTYLRRSLGGS-----VAELPTRAEVESVLA
abPPO3   153   -QVIR-------DKQVPILHYK-FIEPTFEG-----------WQTTMRYMIAG----KAAA--FREWTFNMLTNYTWE
abPPO4   143   -EIIK--------LEQVPILRYS-F-DPSFNGY----------WKTTVRNLIGK----DLEA--TREKTYNMLFNANWE
                :         *           .                    :            . .
```

```
hsTYR    324   LTQYESGSMDKAANFSFRNTLEGFASPLTGIADASQSSMHNALHIYMNGTMSQVQGSANDPIFLLHHAFVDSIFEQWLRR
hsTYRP1  339   VGLFDTPPFYSNSTNSFRNTVEGYSDP-TGKYDPAVRSLHNLAHLFLNGTGGQTHLSPNDPIFVLLHTFTDAVFDEWLRR
scTYR    162   ISAYDLPPYNSASE-GFRNHLEGWRG----------VNLHNRVEVWVGGQMAT-GVSPNDPVFWLHHAYVDKLWAEWQRR
abPPO3   240   ---------LFSNSLEM--------------------VHNTVHFLIGGHMGSVPHAAFDPIFWMHHCNVDRLLALWQTM
abPPO4   232   ---------AFSNSLEA--------------------VHDDIHGFVGGHMTHALFAAFDPIFWLHHSNVDRHLSLWQAL
                :*:    *   ..*              :.  **:*  :   *    .*       *
```
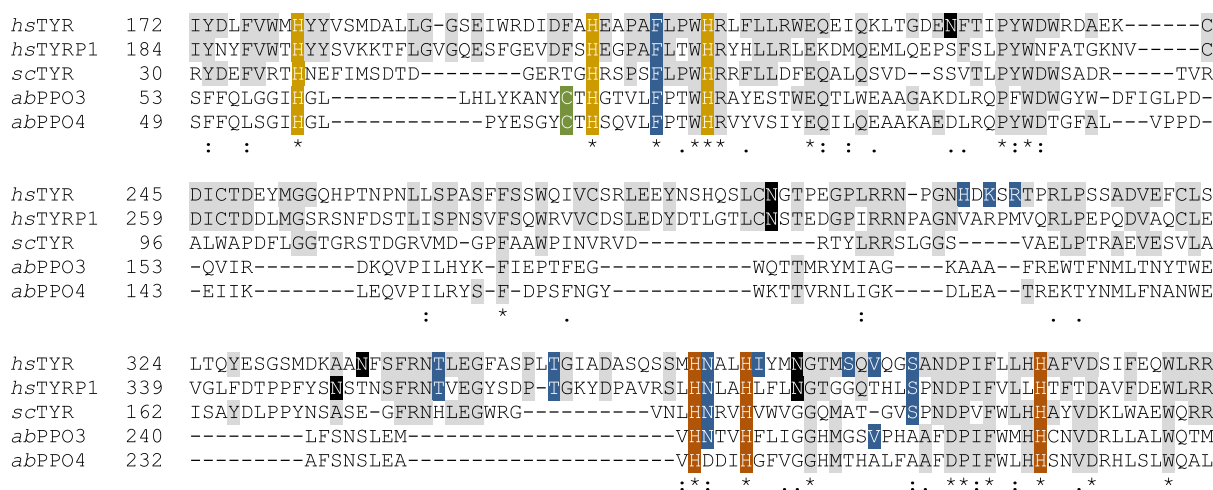
Figure 2. Multiple sequence alignment between *hs*TYR, human TY-related protein 1 (*hs*TYRP1), *Streptomyces castaneoglobisporus* TY (*sc*TYR), and *Agaricus bisporus* TY isoforms PPO3 (*ab*PPO3) and PPO4 (*ab*PPO4): in yellow, histidine residues bound to Cu_A/Zn_A; in orange, histidine residues bound to Cu_B/Zn_B; in black, glycosylation positions; in green, cysteines responsible for the formation of a thioether bond at the active site; in blue, residues predicted to interact with *hs*TYR inhibitors through molecular modeling studies; in light gray, residues of *hs*TYR conserved in the other enzymes.

more efficient immunotherapies. However, no clinical practice or clinical trials related to the use of melanogenesis inhibitors in melanoma therapy have been reported to date, conveying the impression of an unmet potential. The field is still in the early stages of development, and thus only preliminary data are available, involving melanoma cells in *in vitro* experiments and often suboptimal *hs*TYR inhibitors (e.g., kojic acid). Nonetheless, the first results are very promising, and undoubtedly, the discovery of genuine, efficient, and safe *hs*TYR inhibitors will help to foster clinical developments following these pioneer studies.

Controversial Involvement in Neuromelanin Synthesis and Parkinson's Disease. Besides its role in peripheral (cutaneous and ocular) melanogenesis, *hs*TYR could play a central role in the synthesis of neuromelanin in the brain. Neuromelanin is a dark pigment incorporating eumelanin and pheomelanin components, covalently bound to lipids and peptides and present in dopaminergic neurons of the brain region substantia nigra (SN).[28] In a way similar to melanins, neuromelanin acts as a double-edged sword, on the one hand delivering radical scavenging, antioxidant, toxic metal binding, and toxins sequestering properties to particularly exposed catecholaminergic neurons but on the other hand potentially causing dopaminergic neuron degeneration and ultimately Parkinson's disease (PD).[29] Because only small amounts of mRNA coding for *hs*TYR, and of *hs*TYR itself were found in human SN,[30,31] the role of the enzyme in neuromelanin synthesis has long been controversial. However, *hs*TYR is able to catalyze not only the conversion of L-tyrosine and L-DOPA but also the oxidation of the dopamine catechol ring ($K_m = 16$ mM, $k_{cat} = 61$ s^{-1}),[2] an essential step in the pathway of neuromelanin production.[32,33] The aggregation of α-synuclein, a key event in PD pathogenesis, may be promoted by the oxidative action of *hs*TYR on the exposed Y39 residue of the peptide.[34] In addition, a clear relationship between PD and cutaneous melanoma has been established. While most cancers are less frequent in PD patients, melanoma is found at an increased incidence compared with the general population; patients with PD have ~2- to 4-fold increased risk of developing melanoma and vice versa.[35] Interestingly, melanocytes and neurons from

SN are both pigmented and derived from neuroectodermal cells and may share protein biosynthesis and regulation pathways. In a recent study, the overexpression of *hs*TYR in SN from rats induced an age-dependent synthesis of neuromelanin, showing accumulation levels similar to elderly humans while causing the emergence of an age-dependent PD phenotype.[36] These results suggest that intracellular neuromelanin accumulation may be responsible for PD initiation and could open new options of treatment based on the modulation of neuromelanin level. However, the inhibition of neuromelanin synthesis, for example, through *hs*TYR targeting, could also trigger health issues. Indeed, the rare loss-of-function V275F mutation of *hs*TYR, associated with albinism, is more common in PD cases, unveiling a link between *hs*TYR inactivation and neurodegeneration.[37] Altogether, the previously described elements advocate for a major role of *hs*TYR not only in neuromelanin production (for better or for worse) but also in the emergence of PD. As such, inhibiting neuronal *hs*TYR action could be a promising exploratory therapeutic axis for PD. But it is essential to consider that a tight regulation of neuromelanin level, between its protective and pathogenic thresholds,[36] is needed and probably challenging.

Tyrosinase and Alkaptonuria-Related Ochronosis. Finally, a potential implication of *hs*TYR in the ochronosis occurring in alkaptonuria has been recently suggested.[38] Alkaptonuria is a rare disease caused by an inactivating mutation in the gene coding for homogentisate 1,2-dioxygenase (HGD), an enzyme able to convert homogentisic acid (HGA), a *p*-diphenol intermediate in L-tyrosine metabolism, into linear products by phenyl ring oxidation. While young patients manage to excrete the gram quantities of HGA produced daily through urine, the deterioration of renal function with age induces an accumulation in various tissues. Yet, an oxidation of HGA into a benzoquinone acetic acid occurs, with a subsequent polymerization into ochronotic pigment, following a process remarkably similar to melanogenesis, termed ochronosis.[39] The ochronotic pigment causes a dark blue deposition in skin, cartilages, tendons, ligaments, eyes, ears, heart, arterial system, or bones, and its progression is associated with rapid tissue destruction, debilitating clinical sequelae, and ultimately death.[40] The
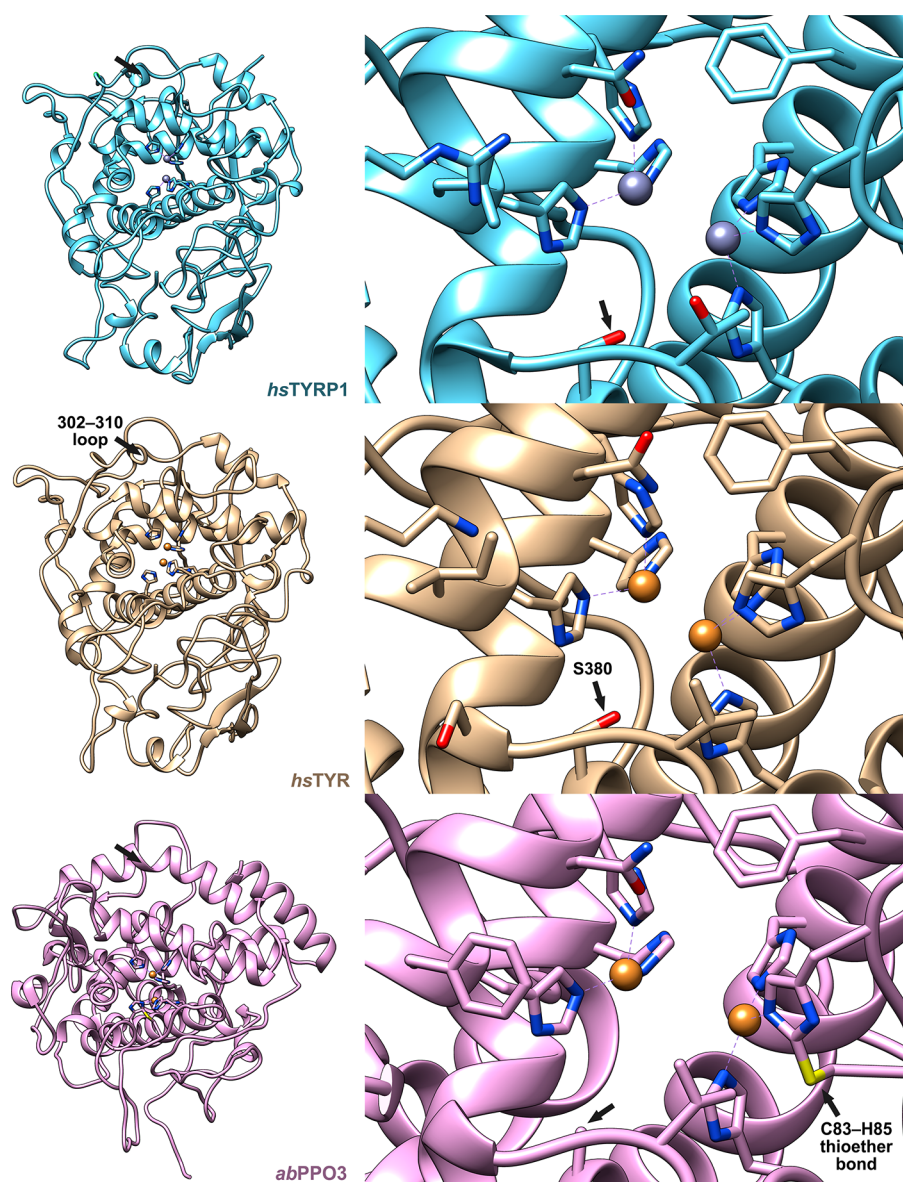
Figure 3. Visual representations (global structure and active-site closer view) of a crystal structure of *hs*TYRP1 (PDB code 5m8l),[50] a homology model of *hs*TYR,[49] and a crystal structure of *ab*PPO3 (PDB code 2y9w).[48]

oxidation of HGA could be catalyzed by *hs*TYR, given the nonspecific action of the enzyme, paving the way to ochronosis appearance.[38] Indeed, TYRs are able to oxidize *p*-diphenols, such as hydroquinone, in certain conditions, especially in a medium rich in catechols, such as ʟ-DOPA.[41] If the involvement of *hs*TYR in the disease is confirmed in the future, the inhibition of the enzyme activity could provide a therapeutic option for preventing ochronosis in the context of alkaptonuria, even if it would only treat an undesirable symptom and not the genetic disease itself.

◼ TYROSINASE-TARGETING DRUG DISCOVERY FOR HUMAN APPLICATIONS

Mushroom Tyrosinase as a Deceptive Model. In the literature devoted to TYR inhibitors, a general assumption prevails implicitly (and sometimes explicitly) that molecules identified through mushroom tyrosinase assays should be potential TYR inhibitors for human-directed applications, i.e., *hs*TYR inhibitors. Indeed, TYR from the white button mushroom *Agaricus bisporus* (*ab*TYR, actually composed of six isoforms, i.e., *ab*PPO1−6, the two most abundant being *ab*PPO3 and *ab*PPO4 by far[42]) has been readily available at low cost from commercial sources for several decades, while *hs*TYR is still costly and hard to produce in a proper form (*vide infra*). Thus, the large majority of TYR-targeting compounds so far were identified on the exclusive basis of anti-*ab*TYR activity, and a considerable pool of several thousand *ab*TYR inhibitors is known, including very diverse structures and a lot of natural products.[13] Even the emblematic kojic acid, widely used in human dermocosmetics, was originally discovered as an *ab*TYR inhibitor, through a phytochemistry study in 1979.[43] However, *ab*TYR and *hs*TYR are actually very different. While *ab*TYR is a soluble oligomeric enzyme found in the cytosol, *hs*TYR is a highly glycosylated monomeric protein anchored in the melanosome membrane. In addition, mammalian TYRs have only 22−24% overall identity with *ab*TYR in a region of 48−49% sequence coverage.[2] The human enzyme contains a unique cysteine-rich subdomain located at the cytosol of melanosomes

(the EGF domain), a transmembrane hydrophobic domain, and seven asparagine glycosylation sites (N86, N111, N161, N230, N290, N337, N371, Figure 2), three features completely absent from abTYR.[44] Even at the active site, major differences were noticed. Even if the dicopper center surrounded by six histidines is conserved, the second sphere of coordination does greatly vary. Especially, some hot spot residues located near the hsTYR active site that were predicted to establish crucial direct interactions with some of the more efficient hsTYR inhibitors reported to date (*vide infra*),[45−47] such as H304, K306, R308, T343, T352, I368, S375 or S380, are totally absent from abPPO3 and abPPO4 (Figure 2). These divergences seen upon sequence comparison have been substantiated in the light of three-dimensional structure examination. Especially, considering the crystal structure of abPPO3[48] and a homology model of hsTYR based on hsTYRP1 as a template,[49,50] key variations appear. For example, a covalent thioether bond occurs between a cysteine and a copper-chelating histidine residue in abTYR (C83 and H85 in abPPO3,[48] C80 and H82 in abPPO4 (Figure 2),[51] as confirmed by the corresponding crystal structures (Figure 3)), a characteristic highly conserved among plant and fungal PPOs and TYRs but not in hsTYR. This absence could be involved in the significant conformational changes observed. Near the active site, residues 302−310 are part of a very flexible loop in hsTYR and seem to potentially interact with extended molecules chelating the dicopper center. In abPPO3, as well as in abPPO4 and hsTYRP1, this portion is structured as a more rigid α-helix, making similar contacts irrelevant (Figure 3). This could constitute a major difference in interaction patterns, in particular for bigger inhibitors. Another important discrepancy is the absence in abPPO3 and abPPO4 of hsTYR residue S380 in the immediate vicinity of the dicopper center, while it is conserved in hsTYRP1 as S394. This amino acid may be involved in substrate activation, thus controlling hsTYR action, as witnessed by the dramatic decrease in enzymatic activity observed for S380A and S380P mutations.[52] The latter has been associated with type 1 oculocutaneous albinism (OCA1) through a complete suppression of monophenolase activity, jeopardizing the melanogenesis process in patients.[53] Thus, S380 may also exert a crucial influence in hsTYR inhibitor binding (Figure 3). As a consequence, many abTYR inhibitors give unsatisfactory results when tested against hsTYR, an observation that includes some of the most widely used depigmenting agents currently employed as dermocosmetics. Regarded as reference molecules and used as standards for TYR inhibition, kojic acid, hydroquinone, or arbutin actually shows minimal effect against the human enzyme, with inhibition values 100-fold or 1000-fold higher than those from abTYR-based assays (Table 1). Even rucinol, which exhibits a significant anti-hsTYR activity (IC_{50} = 21 μM), inhibits abTYR in a far more efficient way (IC_{50} = 0.6 μM). This global inefficiency leads to the use of high concentrations of skin-whitening agents such as kojic acid and hydroquinone in dermatological preparations, thereby promoting the widely recorded adverse effects previously mentioned. Therefore, a development process involving an appropriate array of tests performed using human models appears as a requirement, and studies relying only on abTYR-based assays and assuming a smooth transposition to the human enzyme should be avoided.

Novel Human Tyrosinase-Based Strategies for Depigmenting Agents Discovery. The ubiquity of abTYR-based assays in the literature originates from difficulties traditionally encountered in hsTYR production. The maturation of hsTYR is

Table 1. Comparison of Activity of Selected TYR Inhibitors against Isolated Mushroom (abTYR) and Human (hsTYR) TYRs

inhibition value	TYR inhibitor	activity vs abTYR (μM)	activity vs hsTYR (μM)
K_i	kojic acid[2]	4.3	350
	benzoic acid[2]	4.6	520
	2-hydroxypyridine N-oxide[45,54]	1.8	128
IC_{50}	kojic acid[46,55]	6.0	500
	hydroquinone[46,55]	1.1	4400
	arbutin[46,55]	40	6500
	resorcinol[47,56]	652	>3000
	rucinol[46,55]	0.6	21
	4-hexylresorcinol[46,55]	1.2	94
	4-phenylethylresorcinol[46,55]	0.3	131
	dimethoxytolylpropylresorcinol[46]	0.24	na[a]
	aesculetin[2]	4.3	na[a]

[a]No activity observed at saturation.

indeed a complex process involving heavy and heterogeneous post-translational modifications, a transmembrane anchor, and a trafficking through the endoplasmic reticulum and Golgi, controlled by six or seven specific N-glycans and by copper uptake. Attempts were first made to produce hsTYR from natural sources, but heavy contamination with large amounts of melanin generally thwarted direct purifications from pigmented cell extracts.[57] Nonetheless, several works have reported the purification of hsTYR from human melanotic melanoma metastases (entries 1 and 2, Table 2),[58,59] but the native form of the protein is questionable and the method is not suitable for regular hsTYR production, as it needs biological tissues retrieved from patients by surgery. Thus, the heterologous recombinant expression of hsTYR in nonmelanogenic cells was considered. Kong et al. reported two bacterial hsTYR expression systems involving *E. coli* and managed to obtain the full-length enzyme and the melanosomal domain, both with good TYR activity (entries 3 and 4, respectively, Table 2); the melanosomal domain yielded a dubious K_m value for L-tyrosine however.[60,61] Several research teams have tried to replicate these constructs and failed systematically,[2,57,62] casting doubt over the method. Indeed, the hsTYR glycosylation pattern is unavailable in simple organisms such as *E. coli* for the production of properly matured recombinant enzyme. Yet, it was shown that N-glycans are crucial for maintaining the folding and catalytic activity of hsTYR.[63] However, if N86 and N371 glycosylation sites seem to be mandatory for maintaining a decent enzymatic activity, N230 and N337 N-glycans appear as more dispensable, as the N230Q/N337Q double mutant successfully retained full wild-type activity.[64] This was confirmed by partial deglycosylation of hsTYR construct 5 though PNGase F action, yielding an active form of hsTYR with kinetic properties comparable to other reported hsTYR obtained from different sources (construct 7 from Table 2 and enzymes isolated from melanoma cells).[2] Studies thus focused on the production of (at least partially) glycosylated hsTYR in more elaborate expression systems. Using a baculovirus expression system, Fogal et al. managed to produce full-length hsTYR in insect cells (from *Spodoptera frugiperda*).[2] Another group reported the expression of both the melanosomal domain and the full-length protein using insect larvae (from *Trichoplusia ni*) infected with a baculovirus, as expression host.[62,65] Both works yielded constructs with activity and kinetic

Table 2. Native and Recombinant Expression Systems for *hs*TYR with Estimated Molecular Weights, Lengths, Michaelis–Menten Constants, and Estimated Yields

	source	MW (kDa)	construct length	K_m (mM), L-DOPA	K_m (mM), L-tyrosine	yield (mg/L)
1	human melanoma metastasis[58]	~67	native			0.2[a]
2	human melanoma metastasis[59]	~53	native	0.20		1.1[a]
3	E. coli[60]	~66	1–529	0.36	0.17	1
4	E. coli[61]	~52	19–474	0.34	0.0013	3.8
5	insect S. frugiperda Sf9 cells[2]	~66	1–513	0.34	0.22	8
6	insect T. ni High Five cells[44]	~60	19–456			4–6
7	insect T. ni larvae[62]	~57	19–469	0.46	0.16	>1[a]
8	insect T. ni larvae[65]	~70	1–529	0.67	0.09	
9	human HEK cells[57]	~70	1–511	0.51		
10	human HEK cells[57]	~57	1–438	0.50		15.6

[a]Per 10 g of biomass.
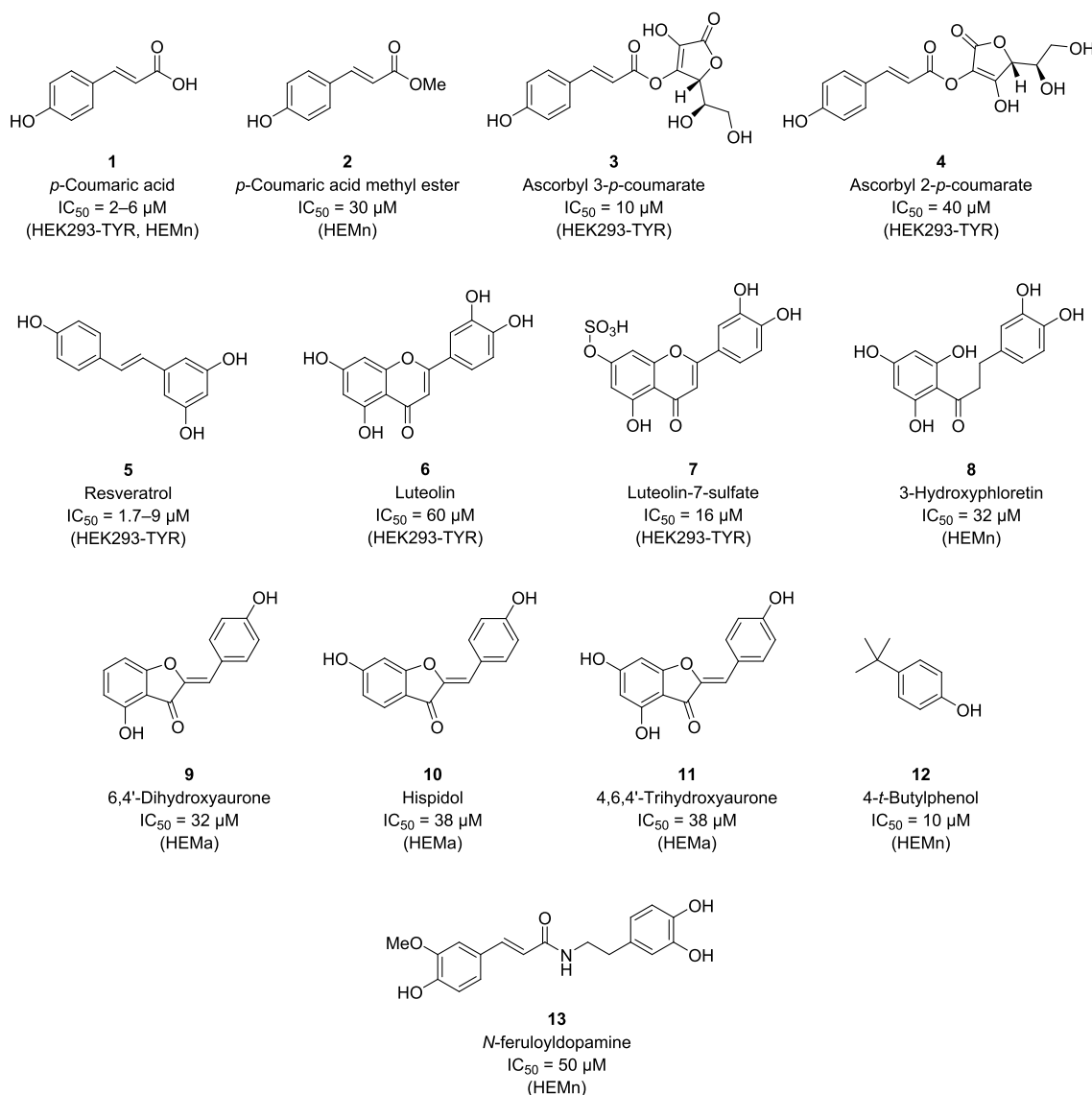
Figure 4. Structure and activity of 4-phenol and 3,4-catechol derivatives (with a unique substituent at *para* position of one OH group) as *hs*TYR inhibitors identified through cell-free crude extract assays. In parentheses are the cell lines employed in the study.

constants comparable to those from the literature and with compatible glycosylation levels, although only paucimannose structures are produced by insects, vs more complex *N*-glycans by mammals.[2] The production of *hs*TYR in nonmelanogenic human cells, i.e., HEK cells, was described by another team.[57]

While in nonmelanogenic mammalian cells the overexpression of *hs*TYR was often rapidly associated with intracellular melanin accumulation, resulting in growth interruption and cell death, HEK cells were found to readily secrete a truncated variant of the enzyme. Thus, a total of eight constructs were produced, with
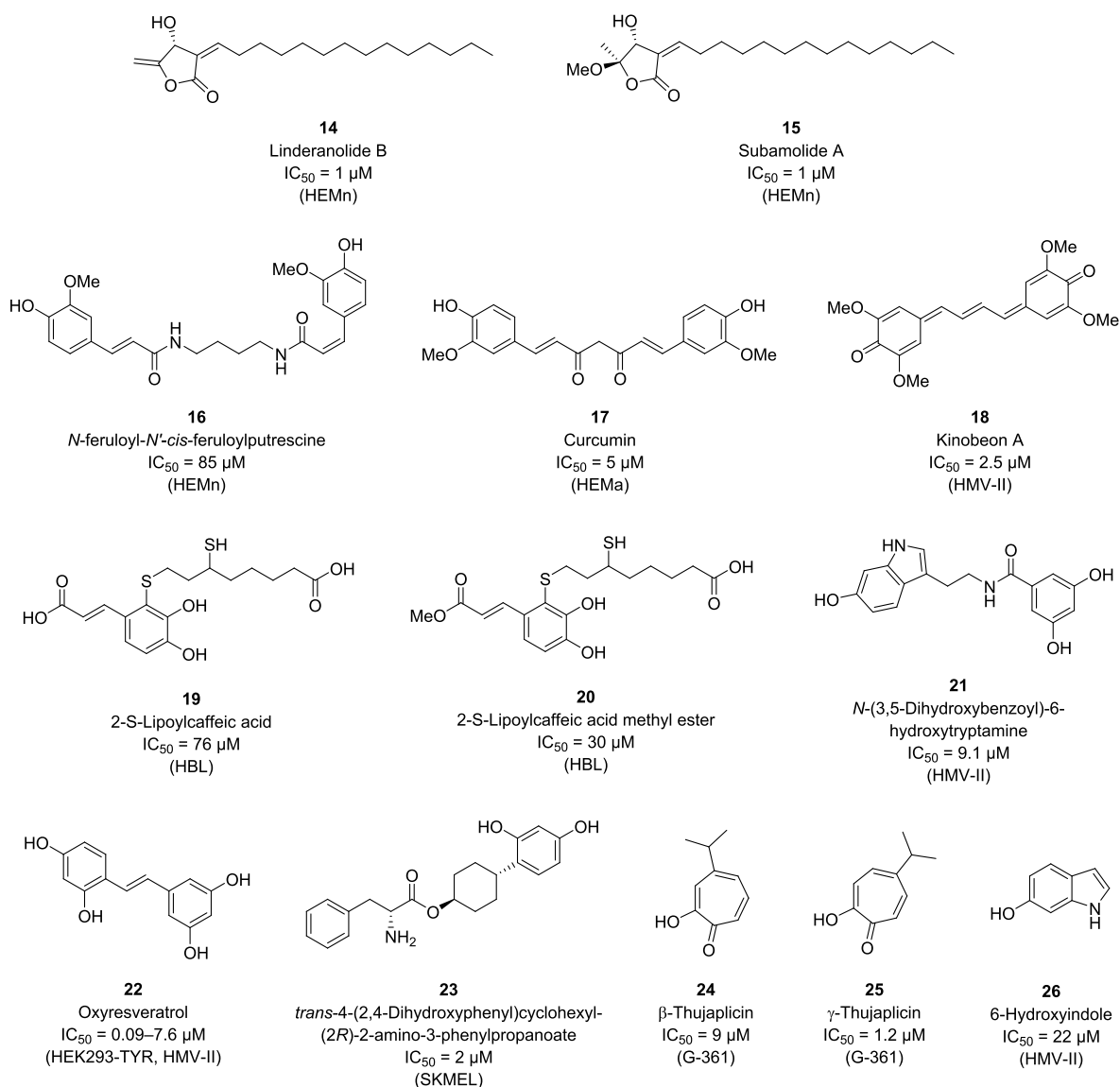
14
Linderanolide B
IC_{50} = 1 μM
(HEMn)

15
Subamolide A
IC_{50} = 1 μM
(HEMn)

16
N-feruloyl-*N'*-*cis*-feruloylputrescine
IC_{50} = 85 μM
(HEMn)

17
Curcumin
IC_{50} = 5 μM
(HEMa)

18
Kinobeon A
IC_{50} = 2.5 μM
(HMV-II)

19
2-S-Lipoylcaffeic acid
IC_{50} = 76 μM
(HBL)

20
2-S-Lipoylcaffeic acid methyl ester
IC_{50} = 30 μM
(HBL)

21
N-(3,5-Dihydroxybenzoyl)-6-hydroxytryptamine
IC_{50} = 9.1 μM
(HMV-II)

22
Oxyresveratrol
IC_{50} = 0.09–7.6 μM
(HEK293-TYR, HMV-II)

23
trans-4-(2,4-Dihydroxyphenyl)cyclohexyl-(2R)-2-amino-3-phenylpropanoate
IC_{50} = 2 μM
(SKMEL)

24
β-Thujaplicin
IC_{50} = 9 μM
(G-361)

25
γ-Thujaplicin
IC_{50} = 1.2 μM
(G-361)

26
6-Hydroxyindole
IC_{50} = 22 μM
(HMV-II)

Figure 5. Structure and activity of other molecules as *hs*TYR inhibitors identified through cell-free crude extract assays. In parentheses are the cell lines employed in the study.

total lengths ranging from 1−511 to 1−428. While some of these constructs led to a catalytic activity drop, the full-length protein (entry 9) and a portion of the melanosomal domain (entry 10, Table 2) showed kinetic values and activities very similar to the literature, with expected native glycosylation patterns.[57] More recently, the large-scale expression of a melanosomal *hs*TYR construct was performed from *T. ni*-derived High Five cells (entry 6, Table 2), with an enhanced secretion of the enzyme induced by a honeybee melittin signal peptide.[44] This work led to promising crystallization results, but only preliminary diffraction data were obtained with a near-atomic resolution of 3.5 Å. Thus, an operable crystal structure of *hs*TYR at atomic resolution is still needed for allowing the rational design of specific inhibitors targeting the human enzyme. While initially most of the molecular modeling experiments were done using crystal structures of mushroom or bacterial TYRs, two relevant and robust homology models of *hs*TYR were disclosed recently, paving the way for more accurate predictions of binding energies and interactions. The first one was built based on structural data from *S. castaneoglobisporus* TYR (*sc*TYR) and *Ipomea batata*

catechol oxidase (*ib*CO).[66] However, since the deciphering of *hs*TYRP1 three-dimensional structure[50] and given the high homology of the protein with *hs*TYR (44% identity), several studies have reported the construction of models using *hs*TYRP1 as the template.[47,52] In particular, one of these models is available in the SwissModel Expasy repository.[49] These recent breakthroughs in the fields of *hs*TYR expression and purification, and of *hs*TYR structure knowledge, enabled the discovery of the first two inhibitors with K_i values below 1 μM, among others, in the past few years.[45,46]

PIONEER GENERATIONS OF TRUE HUMAN TYROSINASE INHIBITORS

Inhibitors of Tyrosinase Activity in Human Cell-Free Crude Extracts. Tyrosinase inhibition belongs to the core set of biological activities traditionally measured for natural extracts and isolated products, along with antioxidant or antibacterial properties. Hence, if many natural TYR inhibitors were identified through *ab*TYR-based assays, a scarcely lesser amount of such molecules were evaluated using cell-free crude extracts of
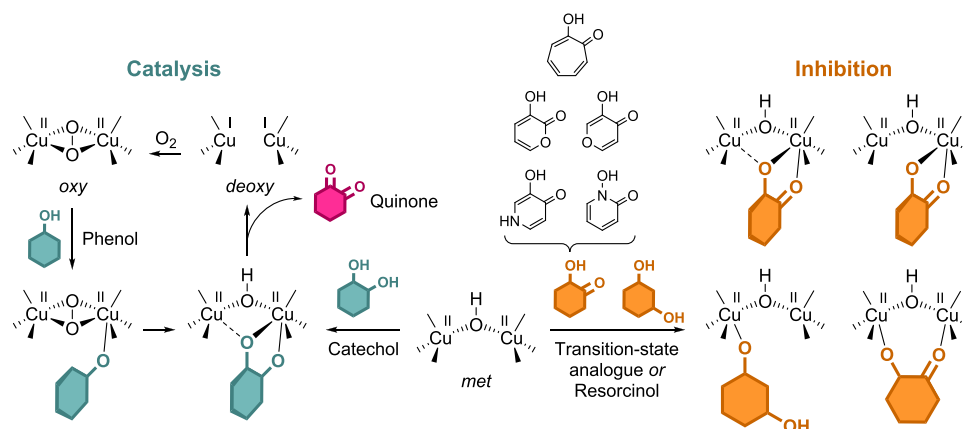
Figure 6. Simplified catalytic cycle of the oxidation of 4-phenols and 3,4-catechols by TYRs, and examples of possible binding modes for nonoxidizable transition-state analogues and resorcinols as active-site inhibitors.

TYR-expressing cell lines. Among the cell lines employed, the B16 and melan-a murine melanoma cells were widely used. However, those cells overexpress mouse TYR (mmTYR) and not hsTYR. Even if the two mammalian TYRs share a good level of homology (>80% identity), potential hot spot residues of hsTYR are missing, such as R308 (K308 in mmTYR). Therefore, studies reporting results obtained in *Mus musculus* were not considered in this review. Besides, a lot of works have focused on measuring the anti-TYR activity of natural products using a variety of hsTYR-overexpressing human cell lines. These include melanogenic human malignant melanoma cells (e.g., G-361, HBL, HMV-II, SKMEL), normal adult or newborn melanocytes (HEMa and HEMn, respectively), and human nonmelanogenic cells transfected with a hsTYR construct (HEK-293-TYR), which readily provide cell-free crude preparations of hsTYR for inhibitor screening. Among the sizable amount of tested natural products and synthetic compounds, only reports describing IC_{50} values below 100 μM are included in this review. A substantial portion of the identified compounds are phenol derivatives, for example, the very simple 4-*tert*-butylphenol (**12**)[67] or 6-hydroxyindole (**26**).[68] Unsurprisingly, L-tyrosine and L-DOPA structural analogues, derived from p-coumaric acid[69,70] and caffeic acid (**1−4, 19, 20**),[71] showed some affinity for hsTYR (Figures 4 and 5). Interestingly, p-coumaric acid itself (**1**) was far more active against crude hsTYR preparations than against abTYR (IC_{50} = 2−6 μM vs >100 μM).[69,70,72−74] Resveratrol (**5**) showed a good IC_{50} value, but its resorcinol-based analogue oxyresveratrol (**22**) was found to be more active (IC_{50} = 0.09−7.6 μM vs 1.7−9 μM), as usually expected from the presence of resorcinol moieties (*vide infra*).[68,73,75,76] Flavonoids and derivatives were also sporadically identified, belonging to flavone (**6, 7**),[77] dihydrochalcone (**8**),[78] and aurone (**9−11**) subclasses,[79] with moderate activities (Figure 4). A larger 3,4-catechol, N-feruloyldopamine (**13**), was also described.[80] Some other extended linear molecules were reported, such as linderanolide B (**14**), subamolide A (**15**, IC_{50} = 1 μM for both),[81] N-feruloyl-N'-*cis*-feruloylputrescine (**16**),[82] curcumin (**17**),[83] kinobeon A (**18**),[84] 2-S-lipoylcaffeic acid (**19**), 2-S-lipoylcaffeic acid methyl ester (**20**),[71] N-(3,5-dihydroxybenzo-yl)-6-hydroxytryptamine (**21**),[68] or *trans*-4-(2,4-dihydroxyphenyl)cyclohexyl-($2R$)-2-amino-3-phenyl-propanoate (**23**)[85] (IC_{50} = 2−85 μM), suggesting that the presence of long chains, either as an internal linker or as a hydrophobic tail, does not prevent hsTYR inhibition (Figure 5). However, molecules from Figure 4 are phenols or catechols

bearing a unique substituent at the *para* position of one OH group (i.e., 4-phenols and 3,4-catechols), which are reminiscent of the structures of natural substrates L-tyrosine and L-DOPA. Given the nonspecific nature of hsTYR catalytic activity, it is thus likely that at least some of them are actually substrates and not inhibitors, as in the conditions of the tests usually performed, the concomitant oxidation of the anti-hsTYR agent is often hard to detect. For example, resveratrol (**5**),[86] p-coumaric acid (**1**),[87] hispidol (**10**)[88−90] (all 4-phenols), caffeic acid,[87] and luteolin (**6**)[91] (all 3,4-catechols) have already shown an alternative substrate behavior, instead of genuinely inhibiting the enzyme action, when faced with isolated TYRs from various species (Figure 6, catalysis panel). Yet, the oxidation of depigmenting agents by hsTYR could generate reactive quinones and trigger the formation of potentially toxic polymers or conjugates, a lesson learned from hydroquinone (*vide supra*). Therefore, the development of new active-site binding hsTYR inhibitors through more ambitious medicinal chemistry programs should involve the use of nonoxidizable counterparts to phenols or catechols, such as resorcinol groups and transition-state analogues (Figure 6, inhibition panel). Indeed, if some resorcinols are susceptible to undergo a TYR-mediated slow oxidation in the presence of specific additives,[56] they mostly act as inhibitors in physiological conditions, as confirmed by Mann et al. recently.[46] For their part, transition-state analogues are named after their structural analogy with the catechol substrate and the quinone product of TYR catalytic cycle, but their oxidation state does not allow TYR-mediated enzymatic reaction. As such, they adopt a true inhibitor behavior upon dicopper center binding.[54] In this regard, the work from Yoshimori et al. around thujaplicin isomers (**24** and **25**, Figure 5)[92] was inspirational, the tropolone scaffold embodying the typical nonoxidizable copper-chelating group, ensuring an actual inhibitor behavior.

Inhibitors of Isolated, Purified Human Tyrosinase. As already mentioned, the development of dedicated hsTYR inhibitors appropriately evaluated against the isolated enzyme has long encountered significant roadblocks. Consequently, such molecules have emerged in scientific reports only recently, following the substantial progresses made in hsTYR expression and purification. Globally, two hsTYR constructs (5 and 10 (Table 2)) were used for most anti-hsTYR assays reported. Among the compounds seen as classical TYR inhibitors, only L-mimosine (**28**) and phenylthiourea (**29**) delivered a significant influence on hsTYR catalytic activity (K_i = 10.3 μM and 1.7 μM,
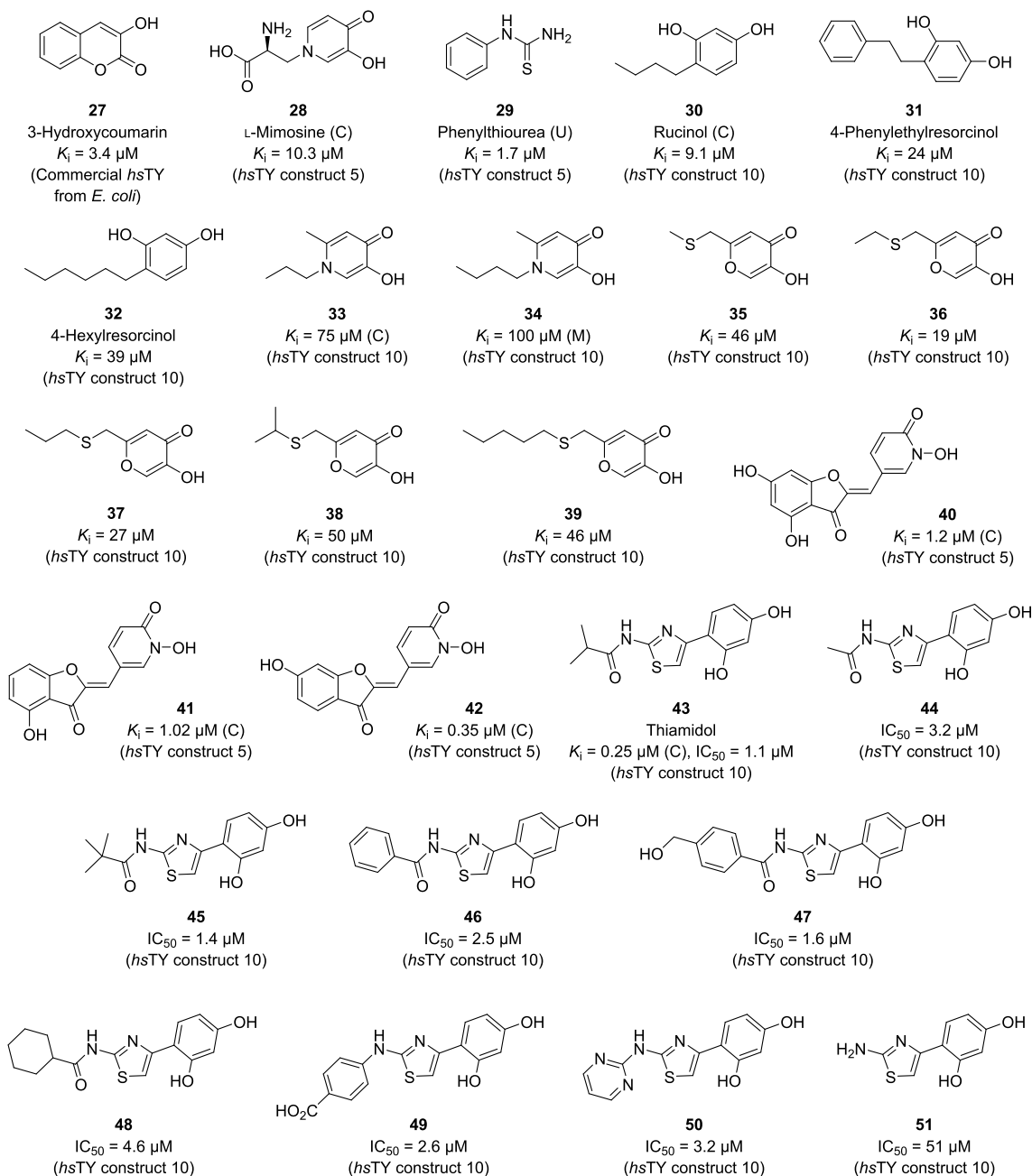
27
3-Hydroxycoumarin
K_i = 3.4 μM
(Commercial hsTY
from *E. coli*)

28
L-Mimosine (C)
K_i = 10.3 μM
(hsTY construct 5)

29
Phenylthiourea (U)
K_i = 1.7 μM
(hsTY construct 5)

30
Rucinol (C)
K_i = 9.1 μM
(hsTY construct 10)

31
4-Phenylethylresorcinol
K_i = 24 μM
(hsTY construct 10)

32
4-Hexylresorcinol
K_i = 39 μM
(hsTY construct 10)

33
K_i = 75 μM (C)
(hsTY construct 10)

34
K_i = 100 μM (M)
(hsTY construct 10)

35
K_i = 46 μM
(hsTY construct 10)

36
K_i = 19 μM
(hsTY construct 10)

37
K_i = 27 μM
(hsTY construct 10)

38
K_i = 50 μM
(hsTY construct 10)

39
K_i = 46 μM
(hsTY construct 10)

40
K_i = 1.2 μM (C)
(hsTY construct 5)

41
K_i = 1.02 μM (C)
(hsTY construct 5)

42
K_i = 0.35 μM (C)
(hsTY construct 5)

43
Thiamidol
K_i = 0.25 μM (C), IC$_{50}$ = 1.1 μM
(hsTY construct 10)

44
IC$_{50}$ = 3.2 μM
(hsTY construct 10)

45
IC$_{50}$ = 1.4 μM
(hsTY construct 10)

46
IC$_{50}$ = 2.5 μM
(hsTY construct 10)

47
IC$_{50}$ = 1.6 μM
(hsTY construct 10)

48
IC$_{50}$ = 4.6 μM
(hsTY construct 10)

49
IC$_{50}$ = 2.6 μM
(hsTY construct 10)

50
IC$_{50}$ = 3.2 μM
(hsTY construct 10)

51
IC$_{50}$ = 51 μM
(hsTY construct 10)

Figure 7. Structure and activity of *hs*TYR inhibitors identified through isolated enzyme inhibition assays. In parentheses is the *hs*TYR construct employed in the study (Table 2). Additional letters in parentheses correspond to competitive (C), uncompetitive (U), and mixed (M) inhibition mechanisms, where determined.

respectively), whereas kojic acid, hydroquinone, or arbutin showed almost inactive profiles (Table 1).[2,46] Besides, several derivatives including various nonoxidizable copper-chelating moieties, such as 3-hydroxy-2*H*-pyran-2-one, 3-hydroxypyridin-4(1*H*)-one, 3-hydroxy-4*H*-pyran-4-one, 1-hydroxypyridin-2(1*H*)-one, or 2,4-resorcinol, were described, with uneven results (Figure 6 and Figure 7).[45−47,93,94] Indeed, while kinetic analyses for L-mimosine (**28**), rucinol (**30**), and compounds **33**, **34**, and **40−43** suggested at least partial active-site binding (they were found to act as strict competitive or mixed inhibitors), as expected from the introduction of copper-chelating groups, the inhibition potency recorded was mostly dependent on the rest of the structure. The introduction of simple aliphatic chains, either directly or through thioether formation, on 3-hydroxypyridin-

4(1*H*)-one and 3-hydroxy-4*H*-pyran-4-one moieties only yielded moderately active molecules but with significant differences. Compound **36** was thus found to be more active (K_i = 19 μM) than homologous **35** and **37−39** (K_i = 27−50 μM),[93] all of them being far more efficient than kojic acid (K_i = 350 μM, Table 1), although based on the same copper-binding scaffold. Embedding 1-hydroxypyridin-2(1*H*)-one or 2,4-resorcinol groups on aurone and thiazole-based scaffolds afforded far more active analogues, with K_i values dropping below 1 μM. Aurone **42** and thiamidol **43**, with K_i = 0.35 μM and 0.25 μM, respectively, are thus the best inhibitors of *hs*TYR discovered to date, among several less potent derivatives (aurones **40** and **41**, and thiazoles **44−51**, Figure 7).[45−47] Interestingly, **42** was conceived by rational design using a *hs*TYR
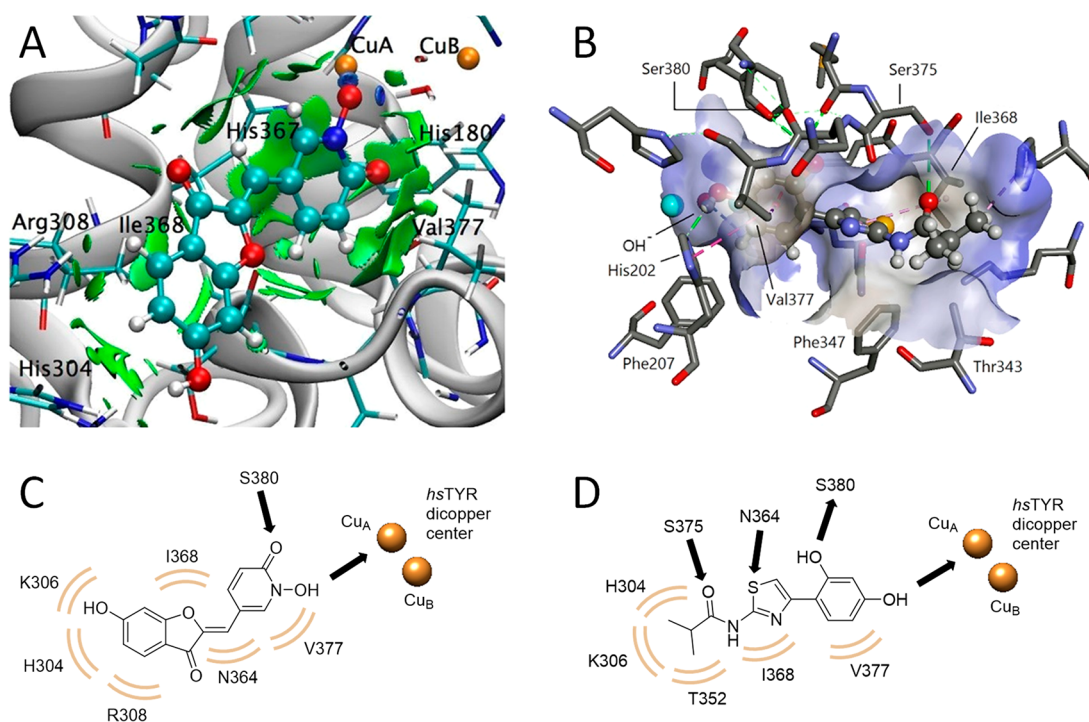
Figure 8. Molecular modeling and interaction patterns. (A) Predicted pose obtained for compound **42** through QM/MM experiments using a homology model of *hs*TYR. Reproduced from ref 45 (Copyright 2017 American Chemical Society). (B) Predicted pose obtained for compound **43** (thiamidol) through molecular docking using a homology model of *hs*TYR. Reproduced from ref 46 (Creative Commons, CC BY-NC-ND 4.0 license). (C) Schematic view of **42**−*hs*TYR interaction pattern. (D) Schematic view of **43**−*hs*TYR interaction pattern. Arrows represent hydrogen bonds. Golden circular arcs represent hydrophobic interactions.

homology model and a transition-state analogue (1-hydroxypyridin-2(1*H*)-one) previously scrutinized for its interactions with TYRs and model complexes,[54] while **43** was selected from a screen of 50 000 compounds and appropriately modified, indicating that both strategies are valid and probably complementary. Indeed, if a very active aurone analogue (**42**) was readily identified among only three compounds rationally conceived (revealing the deleterious effect of the phenol group at position 4 (K_i = 1.2 μM for **40** vs 0.35 μM for **42**)), the thiazole series was far more fine-tuned. Starting from the initial hit **51** (IC$_{50}$ = 51 μM), alkylation or acylation of the amino group yielded respective "amines" and "amides" lines of compounds. First, it was shown that only the 2,4-resorcinol moiety led to efficient *hs*TYR inhibition, among other phenol, catechol, and resorcinol patterns. Second, the thiazole ring was found to be far more beneficial than imidazole, phenyl, or inverted thiazole counterparts. Third, while the substitution of the 2-amino group appeared to have lower influence on the activity, the "amides" line was generally associated with a 4- to 20-fold better efficiency. In addition, small substituents are usually preferred over larger and bulkier hydrophobic groups (e.g., IC$_{50}$ = 1.1 μM and 1.4 μM for **43** and **45** vs 2.5 μM and 4.6 μM for **46** and **48**). In both studies, molecular modeling experiments were undertaken for unraveling ligand−protein interactions at the active site of *hs*TYR via ligand docking, or more robust QM/MM approaches, as an accurate simulation of ligand−copper interactions is a major issue. Compounds **42** and **43** were found to bind to a single copper atom, i.e., Cu$_A$, through an OH group (either an N−OH or a phenol group), while interacting with hot spot residues V377 and S380, located at the direct vicinity of the dicopper center (Figure 8). Crucial interactions were also spotted with distant residues, such as I368

or T352. In addition, thiamidol **43** was shown to accept two hydrogen bonds between S375 and the amide carbonyl and between N364 and the sulfur atom of the thiazole ring. Finally, both molecules seem to interact with the 302−310 loop of *hs*TYR (Figure 3) (especially with H304, K306, and R308), a flexible part of the protein located relatively far from the dicopper center that is not conserved in *hs*TYRP1 and thus probably less accurately modeled (Figure 2). Nonetheless, as compounds **42** and **43** were found more active against *hs*TYR than against *ab*TYR (with a sizable 100-fold gap for **43**) and as smaller molecules conversely very frequently show a better *ab*TYR inhibition potency (Table 1), interactions with the 302−310 flexible loop could be a determinant feature for reaching outstanding *hs*TYR inhibition and selectivity levels. Transposing the comparable anti-*hs*TYR activities of compounds **42** and **43** in cellular or tissue contexts produced very divergent results: thiamidol **43** demonstrated its fully retained ability to act in a MelanoDerm pigmented 3D tissue model (IC$_{50}$ = 0.9 μM vs 1.1 μM against isolated *hs*TYR), but aurone **42** was by contrast far less efficient in preventing melanogenesis in MNT-1 human melanoma cells (IC$_{50}$ = 16.6 μM against MNT-1 lysates and 85.3 μM against whole cells, vs K_i = 0.35 μM against isolated *hs*TYR). Finally, **42** and its 4-hydroxy analogue **40** showed very little cytotoxicity against MNT-1 human melanoma cells (IC$_{50}$ > 500 μM), a crucial element given the safety issues met with existing depigmenting agents. However, to date, only two *hs*TYR inhibitors were further evaluated in clinical assays.

Clinical Applications. Skin whitening is the most obvious clinical application of *hs*TYR inhibitors. Currently, in Europe the most prevalent ingredients found in preparations include clinically approved molecules, such as kojic acid, ascorbic acid, arbutin, lactic acid, glycolic acid, aloesin, salicylic acid, α-lipoic

acid, and nicotinamide (in this frequency order), and clinically forbidden agents, such as corticosteroids, hydroquinone, or tretinoin.[95] As previously demonstrated, all the putative *hs*TYR inhibitors from this list, i.e., kojic acid, arbutin, and hydroquinone, are both harmful and inefficient to inhibit the enzyme (*vide supra*). Thus, in the early 2000s clinical data emerged for a more efficient, not cytotoxic, *hs*TYR inhibitor, i.e., rucinol (**30**, Figure 7), marketed as Iklen. In particular, several studies endorsed the use of 0.3% rucinol preparations, pointing out significant melanogenesis reduction in UVB-induced hyperpigmentations, postlaser pigmented lesions, age spots and freckles, and melasma, after an average treatment of 6–12 weeks, with recorded mild adverse effects such as erythema, dryness, peeling, or desquamation.[96] To reduce these effects, a less concentrated preparation of 0.1% was proposed, using liposome encapsulation for increasing the efficacy while reducing side effects. This cream was considered to be efficient in more than 60% of patients with melasma after a treatment of 8 weeks, and no adverse reactions were observed.[97] More recently, thiamidol **43** (Figure 7), a very potent *in vitro* *hs*TYR inhibitor, was evaluated for its ability to reduce the pigmentation level in clinical studies. A continuous improvement was noticed in the whitening of age spots whitening upon a 12-week 0.1–0.2% thiamidol treatment, with significant results obtained from week 4.[46] Similarly, a 12-week treatment of mild to moderate melasma with 0.2% thiamidol gave promising results, as a modified melasma area and severity index (mMASI) improvement was recorded in 83.9% of cases (vs 25.9% for untreated) and no worsening was observed (vs 12.9% for untreated). A clear effect was already seen after 4 weeks, with significant improvement in 35.5% of cases. These results were especially remarkable when compared with those from patients treated with 2.0% hydroquinone (21.4% improvement after 4 weeks, 60.7% after 12 weeks, but 10.7% of cases showed a worsening).[98] A follow-on international study confirmed the efficiency of thiamidol treatment for facial mild-to-moderate hyperpigmentations via split-face and real-world studies. After 12 weeks of treatment, mean skin evenness, radiance, and smoothness were improved by 93.8%, 94.1%, and 50.0%, respectively, and a large majority of patients were responsive (94%, 92.8%, and 78.3%, for the three respective skin parameters). Four-times daily thiamidol application afforded better results than twice daily treatments and was overall very well tolerated by the subjects.[99] Thiamidol finally entered a 200-participants randomized clinical trial in 2019, as a 0.2% cream for treating facial hyperpigmentation (efficacy and tolerability evaluated at weeks 4, 8, and 12).[100] The trial is still ongoing and its completion is expected in December 2020. The claimed goal is to introduce a more efficient depigmenting cream on the cosmetic market. Altogether, these results testify to the potential of new dedicated *hs*TYR inhibitors in clinical applications instead of currently used inefficient and harmful agents.

■ CONCLUSION AND PROSPECTS

The design of true *hs*TYR inhibitors is an appealing research field that has been buoyed by the recent advances made in the unraveling of *hs*TYR involvement in several pathologies, in the protein recombinant expression, solubilization, and purification, and in structural biology and crystallography. Thus, the first anti-*hs*TYR agents have been reported in the past few years, heralding the end of the historically unrivaled dominance of *ab*TYR-oriented studies and affording promising clinical data against age spots and melasma. In parallel, the acquired accurate knowledge

of the catalytic cycle and substrate specificity of the enzyme should lead to a paradigm shift in the choice of copper-chelating groups. Therefore, in light of these recent trends, several recommendations may be proposed for the design and evaluation of novel anti-*hs*TYR agents. First, it becomes obvious that a sole *ab*TYR inhibition measurement should never lead to a direct assumption regarding *hs*TYR inhibition activity; a square puzzle piece does not necessarily fit into a flower-shaped cavity. Compounds designed for human-directed applications should at least be tested against *ab*TYR and a cell-free crude extract of an appropriate *hs*TYR-expressing cell line, such as human melanoma cells, human melanocytes, or transfected non-melanogenic human cells. Ideally, a direct measure of *hs*TYR inhibition activity performed against an isolated enzyme construct would deliver precious kinetic data, revealing the mechanism of action and giving clues about the binding site. Second, in the general frame of TYR inhibition, the development of phenyl analogues bearing 4-hydroxy or 3,4-dihydroxy patterns should be avoided, since they could likely act as alternative substrates rather than as inhibitors, producing quinones similar to those obtained from L-tyrosine and L-DOPA. As in the case of hydroquinone, these reactive species could polymerize or generate conjugates with various cellular nucleophiles, potentially entailing undesired systemic toxicity. For active-site targeting, the use of transition-state analogues and resorcinols that mimic the structure of the naturally oxidized phenolic rings but are resistant to *hs*TYR-mediated oxidation has already provided very promising results. Among them, 3-hydroxy-2*H*-pyran-2-one, 3-hydroxypyridin-4(1*H*)-one, 3-hydroxy-4*H*-pyran-4-one, 1-hydroxypyridin-2(1*H*)-one, or 2,4-resorcinol have afforded efficient *hs*TYR inhibitors, with $K_i < 0.35$ μM in two cases, and pure competitive behaviors. Third, a relevant conception of *hs*TYR ligands using molecular modeling needs appropriate methods and tools for metalloenzymes. Especially, for active-site inhibitors the description of copper–ligand interactions should be accurate enough, as several binding modes are often conceivable (Figure 6, inhibition panel) and as it partially determines the orientation of the molecule and its ability to reach crucial interactions. Conventional docking tools are generally not parametrized for the description of ligand–metal interactions, and the inclusion of a quantum part within QM/MM calculations is thus recommended. Fourth, a particular attention should be paid to molecular interactions with the second sphere of coordination of *hs*TYR dicopper center and with remote residues, including those from the 302–310 flexible loop. H304, K306, R308, T343, T352, N364, I368, S375, V377, and S380 were especially pinpointed for their crucial interactions with compounds **42** and **43**. Among them, only N364 and V377 are conserved in *ab*TYR (and only in isoform *ab*PPO3), underlining the crucial importance of using robust *hs*TYR-based structural data for molecular modeling. The recent release of *hs*TYRP1 crystal structure has offered for this purpose an unprecedented opportunity, allowing the build of far more rigorous homology models. However, some shortcomings still remain, such as the modeling of H304, K306, and R308, all absent from *hs*TYRP1. Overall, the accuracy of *in silico* conception and the availability and relevance of assays using purified constructs will strongly rely on future advances in *hs*TYR crystallography and in *hs*TYR large-scale production. Hopefully such studies will mushroom in the next few years.

■ AUTHOR INFORMATION

Corresponding Author

Romain Haudecoeur − *Département de Pharmacochimie Moléculaire (DPM), UMR 5063, Université Grenoble Alpes, 38041 Grenoble, France;* ⦿ orcid.org/0000-0002-6271-4717; Email: Romain.Haudecoeur@univ-grenoble-alpes.fr

Authors

Brayan Roulier − *Département de Pharmacochimie Moléculaire (DPM), UMR 5063, Université Grenoble Alpes, 38041 Grenoble, France*

Basile Pérès − *Département de Pharmacochimie Moléculaire (DPM), UMR 5063, Université Grenoble Alpes, 38041 Grenoble, France*

Complete contact information is available at:
https://pubs.acs.org/10.1021/acs.jmedchem.0c00994

Notes

The authors declare no competing financial interest.

Biographies

Brayan Roulier obtained his Master's degree in Chemical Biology at University of Strasbourg (France) in 2018. He is currently doing his second year Ph.D. studies at Université Grenoble Alpes (France) under the supervision of Dr. Romain Haudecoeur and Dr. Basile Pérès. He works on the design, synthesis, and biological evaluation of new human tyrosinase inhibitors and related chemical tools for human-directed diagnostic and therapeutic applications.

Basile Pérès obtained his Ph.D. in Medicinal Chemistry from University of Lille 2 (France) in 2006, under the supervision of Prof. Daniel Lesieur and Dr. Saïd Yous. After having worked at the University of Evry (France) in supramolecular chemistry with Prof. Philippe Guéguan, he joined the group of Dr. Christopher McCurdy at University of Mississippi (U.S.) to study the medicinal chemistry of mitragynine analogues. Back to Europe he worked with UCB pharma as a postdoctoral researcher in Belgium before being hired in 2010 at Université Grenoble Alpes (France) as an Assistant Professor. His research focuses on the design and synthesis of bioactive compounds, fluorescent probes, and vectorization.

Romain Haudecoeur obtained his Ph.D. in Chemical Biology from Université Grenoble Alpes (France) in 2011, under the supervision of Prof. Ahcène Boumendjel. He joined the group of Dr. David Monchaud at the University of Burgundy (Dijon, France) as a postdoctoral associate in the same year. He was then appointed as Researcher in 2012 in the Department of Medicinal Chemistry of Université Grenoble Alpes. His research work essentially focuses on the rational targeting of biological macromolecules, with the aim of developing new bioinspired, bioactive, and smart compounds for modulating the function of proteins such as tyrosinases, viral polymerases, and membrane ABC transporters.

■ ABBREVIATIONS USED

AADC, aromatic ʟ-amino acid decarboxylase; *ab*PPO, polyphenol oxidase from *Agaricus bisporus*; *ab*TYR, mushroom tyrosinase from *Agaricus bisporus*; DHI, 5,6-dihydroxyindole; DHICA, 5,6-dihydroxyindole-2-carboxylic acid; HEM, human epidermal melanocytes; HGA, homogentisic acid; HGD, homogentisate 1,2-dioxygenase; HPD, 4-hydroxyphenylpyruvate dioxygenase; *hs*TYR, human tyrosinase; *hs*TYRP1, human tyrosinase-related protein 1; *ib*CO, catechol oxidase from *Ipomea batata*; mMASI, modified melasma area and severity index; *mm*TYR, mammalian tyrosinase from *Mus musculus*; OCA1, type 1 oculocutaneous albinism; PD, Parkinson's disease; PDT, photodynamic therapy; PNGase F, peptide N-glycosidase F; PPO, polyphenol oxidase; QM/MM, quantum mechanics/molecular mechanics; ROS, reactive oxygen species; *sc*TYR, bacterial tyrosinase from *Streptomyces castaneoglobisporus*; SN, substantia nigra; TAT, tyrosine aminotransferase; TH, tyrosine hydroxylase; TYR, tyrosinase

■ REFERENCES

(1) Olivares, C.; Solano, F. New insights into the active site structure and catalytic mechanism of tyrosinase and its related proteins. *Pigm. Cell Melanoma Res.* **2009**, *22*, 750−760.

(2) Fogal, S.; Carotti, M.; Giaretta, L.; Lanciai, F.; Nogara, L.; Bubacco, L.; Bergantino, E. Human tyrosinase produced in insect cells: a landmark for the screening of new drugs addressing its activity. *Mol. Biotechnol.* **2015**, *57*, 45−57.

(3) Dolinska, M.; Wingfield, P. T.; Young, K. L.; Sergeev, Y. V. The TYRP1-mediated protection of human tyrosinase activity does not involve stable interactions of tyrosinase domains. *Pigm. Cell Melanoma Res.* **2019**, *32*, 753−765.

(4) Ito, S. A Chemist's view of melanogenesis. *Pigm. Cell Res.* **2003**, *16*, 230−236.

(5) Naidoo, L.; Khoza, N.; Dlova, N. C. A fairer face, a fairer tomorrow? A review of skin lighteners. *Cosmetics* **2016**, *3*, 33.

(6) Burger, P.; Landreau, A.; Azoulay, S.; Michel, T.; Fernandez, X. Skin whitening cosmetics: feedback and challenges in the development of natural skin lighteners. *Cosmetics* **2016**, *3*, 36.

(7) Sagoe, D.; Pallesen, S.; Dlova, N. C.; Lartey, M.; Ezzedine, K.; Dadzie, O. The global prevalence and correlates of skin bleaching: a meta-analysis and meta-regression analysis. *Int. J. Dermatol.* **2019**, *58*, 24−44.

(8) Global Industry Analysts (GIA) report. http://cosmetics.specialchem.com/news/industry-news/skin-lightening-products-market-to-reach-usd23-bn-by-2020-global-industry-analysts (accessed Jul 17, 2020).

(9) Habbema, L.; Halk, A. B.; Neumann, M.; Bergman, W. Risks of unregulated use of alpha-melanocyte-stimulating hormone analogues: a review. *Int. J. Dermatol.* **2017**, *56*, 975−980.

(10) Maymone, M. B. C.; Neamah, H. H.; Wirya, S. A.; Patzelt, N. M.; Secemsky, E. A.; Zancanaro, P. Q.; Vashi, N. A. The impact of skin hyperpigmentation and hyperchromia on quality of life: a cross-sectional study. *J. Am. Acad. Dermatol.* **2017**, *77*, 775−778.

(11) Andersen, F. A.; Bergfeld, W. F.; Belsito, D. V.; Hill, R. A.; Klaassen, C. D.; Liebler, D. C.; Marks, J. G.; Shank, R. C.; Slaga, T. J.; Snyder, P. W. Final amended safety assessment of hydroquinone as used in cosmetics. *Int. J. Toxicol.* **2010**, *29*, 274S−287S.

(12) Nordlund, J. J.; Grimes, P. E.; Ortonne, J. P. The safety of hydroquinone. *J. Eur. Acad. Dermatol. Venereol.* **2006**, *20*, 781−787.

(13) Pillaiyar, T.; Namasivayam, V.; Manickam, M.; Jung, S.-H. Inhibitors of melanogenesis: an updated review. *J. Med. Chem.* **2018**, *61*, 7395−7418.

(14) Buitrago, E.; Hardré, R.; Haudecoeur, R.; Jamet, H.; Belle, C.; Boumendjel, A.; Bubacco, L.; Réglier, M. Are human tyrosinase and related proteins suitable targets for melanoma therapy? *Curr. Top. Med. Chem.* **2016**, *16*, 3033−3047.

(15) American Cancer Society, Cancer Facts & Figures 2019. https://www.cancer.org/content/dam/cancer-org/research/cancer-facts-and-statistics/annual-cancer-facts-and-figures/2019/cancer-facts-and-figures-2019.pdf (accessed Jul 17, 2020).

(16) Schadendorf, D.; van Akkooi, A. C. J.; Berking, C.; Griewank, K. G.; Gutzmer, R.; Hauschild, A.; Stang, A.; Roesch, A.; Ugurel, S. Melanoma. *Lancet* **2018**, *392*, 971−984.

(17) McDermott, D.; Lebbé, C.; Hodi, F. S.; Maio, M.; Weber, J. S.; Wolchok, J. D.; Thompson, J. A.; Balch, C. M. Durable benefit and the potential for long-term survival with immunotherapy in advanced melanoma. *Cancer Treat. Rev.* **2014**, *40*, 1056−1064.

(18) Brozyna, A. A.; Jozwicki, W.; Carlson, J. A.; Slominski, A. T. Melanogenesis affects overall and disease-free survival in patients with stage III and IV melanoma. *Hum. Pathol.* **2013**, *44*, 2071−2074.

(19) Espenel, S.; Vallard, A.; Rancoule, C.; Garcia, M.-A.; Guy, J.-B.; Chargari, C.; Deutsch, E.; Magné, N. Melanoma: last call for radiotherapy. *Crit. Rev. Oncol. Hematol.* **2017**, *110*, 13−19.

(20) Brozyna, A. A.; Jozwicki, W.; Roszkowski, K.; Filipiak, J.; Slominski, A. T. Melanin content in melanoma metastases affects the outcome of radiotherapy. *Oncotarget* **2016**, *7*, 17844−17853.

(21) Brozyna, A. A.; VanMiddlesworth, L.; Slominski, A. T. Inhibition of melanogenesis as a radiation sensitizer for melanoma therapy. *Int. J. Cancer* **2008**, *123*, 1448−1456.

(22) Slominski, A.; Zbytek, B.; Slominski, R. Inhibitors of melanogenesis increase toxicity of cyclophosphamide and lymphocytes against melanoma cells. *Int. J. Cancer* **2009**, *124*, 1470−1477.

(23) Sharma, S. K.; Huang, Y.-Y.; Hamblin, M. R. Melanoma Resistance to Photodynamic Therapy. In *Resistance to Photodynamic Therapy in Cancer*; Rapozzi, V., Jori, G., Eds.; Springer International Publishing: Switzerland, 2015; pp 229−246.

(24) Suzukawa, A. A.; Vieira, A.; Winnischofer, S. M. B.; Scalfo, A. C.; Di Mascio, P.; da Costa Ferreira, A. M.; Ravanat, J.-L.; de Luna Martins, D.; Rocha, M. E. M.; Martinez, G. R. Novel properties of melanins include promotion of DNA strand breaks, impairment of repair, and reduced ability to damage DNA after quenching of singlet oxygen. *Free Radical Biol. Med.* **2012**, *52*, 1945−1953.

(25) Sharma, K. V.; Bowers, N.; Davids, L. M. Photodynamic therapy-induced killing is enhanced in depigmented metastatic melanoma cells. *Cell Biol. Int.* **2011**, *35*, 939−944.

(26) Sharma, K. V.; Davids, L. M. Depigmentation in melanomas increases the efficacy of hypericin-mediated photodynamic-induced cell death. *Photodiagn. Photodyn. Ther.* **2012**, *9*, 156−163.

(27) Slominski, A. T.; Carlson, J. A. Melanoma resistance: A bright future for academicians and a challenge for patient advocates. *Mayo Clin. Proc.* **2014**, *89*, 429−433.

(28) Zucca, F. A.; Basso, E.; Cupaioli, F. A.; Ferrari, E.; Sulzer, D.; Casella, L.; Zecca, L. Neuromelanin of the human substantia nigra: an update. *Neurotoxic. Res.* **2014**, *25*, 13−23.

(29) Greco, G. Neuromelanin and Parkinson's Disease. In *Handbook of Neurotoxicity*; Kostrzewa, R. M., Ed.; Springer Science: New York, 2014; pp 913−932.

(30) Xu, Y.; Stokes, A. H.; Freeman, W. M.; Kumer, S. C.; Vogt, B. A.; Vrana, K. E. Tyrosinase mRNA is expressed in human substantia nigra. *Mol. Brain Res.* **1997**, *45*, 159−162.

(31) Greggio, E.; Bergantino, E.; Carter, D.; Ahmad, R.; Costin, G.-E.; Hearing, V. J.; Clarimon, J.; Singleton, A.; Eerola, J.; Hellström, O.; Tienari, P. J.; Miller, D. W.; Beilina, A.; Bubacco, L.; Cookson, M. R. Tyrosinase exacerbates dopamine toxicity but is not genetically associated with Parkinson's disease. *J. Neurochem.* **2005**, *93*, 246−256.

(32) Haining, R. L.; Achat-Mendes, C. Neuromelanin, one of the most overlooked molecules in modern medicine, is not a spectator. *Neural Regener. Res.* **2017**, *12*, 372−375.

(33) Hasegawa, T. Tyrosinase-expressing neuronal cell line as in vitro model of Parkinson's disease. *Int. J. Mol. Sci.* **2010**, *11*, 1082−1089.

(34) Tessari, I.; Bisaglia, M.; Valle, F.; Samori, B.; Bergantino, E.; Mammi, S.; Bubacco, L. The reaction of α-synuclein with tyrosinase. Possible implications for Parkinson's disease. *J. Biol. Chem.* **2008**, *283*, 16808−16817.

(35) Bose, A.; Petsko, G. A.; Eliezer, D. Parkinson's disease and melanoma: co-occurrence and mechanisms. *J. Parkinson's Dis.* **2018**, *8*, 385−398.

(36) Carballo-Carbajal, I.; Laguna, A.; Romero-Gimenez, J.; Cuadros, T.; Bové, J.; Martinez-Vicente, M.; Parent, A.; Gonzalez-Sepulveda, M.; Peñuelas, N.; Torra, A.; Rodriguez-Galvan, B.; Ballabio, A.; Hasegawa, T.; Bortolozzi, A.; Gelpi, E.; Vila, M. Brain tyrosinase overexpression implicates age-dependent neuromelanin production in Parkinson's disease pathogenesis. *Nat. Commun.* **2019**, *10*, 973.

(37) Lubbe, S. J.; Escott-Price, V.; Brice, A.; Gasser, T.; Pittman, A. M.; Bras, J.; Hardy, J.; Heutink, P.; Wood, N. M.; Singleton, A. B.; Grosset, D. G.; Carroll, C. B.; Law, M. H.; Demenais, F.; Iles, M. M.; Bishop, D. T.; Newton-Bishop, J.; Williams, N. M.; Morris, H. R. Rare variants analysis of cutaneous malignant melanoma genes in Parkinson's disease. *Neurobiol. Aging* **2016**, *48*, 222.e1−222.e7.

(38) Taylor, A. M.; Kammath, V.; Bleakley, A. Tyrosinase, could it be a missing link in ochronosis in alkaptonuria? *Med. Hypotheses* **2016**, *91*, 77−80.

(39) Roberts, N. B.; Curtis, S. A.; Milan, A. M.; Ranganath, L. R. The pigment in alkaptonuria relationship to melanin and other coloured substances: a review of metabolism, composition and chemical analysis. *JIMD Rep.* **2015**, *24*, 51−66.

(40) Ranganath, L. R.; Norman, B. P.; Gallagher, J. A. Ochronotic pigmentation is caused by homogentisic acid and is the key event in alkaptonuria leading to the destructive consequences of the disease−A review. *J. Inherited Metab. Dis.* **2019**, *42*, 776−792.

(41) Deri, B.; Kanteev, M.; Goldfeder, M.; Lecina, D.; Guallar, V.; Adir, N.; Fishman, A. The unravelling of the complex pattern of tyrosinase inhibition. *Sci. Rep.* **2016**, *6*, 34993.

(42) Weijn, A.; Bastiaan-Net, S.; Wichers, H. J.; Mes, J. J. Melanin biosynthesis pathway in *Agaricus bisporus* mushrooms. *Fungal Genet. Biol.* **2013**, *55*, 42−53.

(43) Saruno, R.; Kato, F.; Ikeno, T. Kojic acid, a tyrosinase inhibitor from *Aspergillus albus*. *Agric. Biol. Chem.* **1979**, *43*, 1337−1338.

(44) Lai, X.; Soler-Lopez, M.; Wichers, H. J.; Dijkstra, B. W. Large-scale recombinant expression and purification of human tyrosinase suitable for structural studies. *PLoS One* **2016**, *11*, No. e0161697.

(45) Haudecoeur, R.; Carotti, M.; Gouron, A.; Maresca, M.; Buitrago, E.; Hardré, R.; Bergantino, E.; Jamet, H.; Belle, C.; Réglier, M.; Bubacco, L.; Boumendjel, A. 2-Hydroxypyridine-*N*-oxide-embedded aurones as potent human tyrosinase inhibitors. *ACS Med. Chem. Lett.* **2017**, *8*, 55−60.

(46) Mann, T.; Gerwat, W.; Batzer, J.; Eggers, K.; Scherner, C.; Wenck, H.; Stäb, F.; Hearing, V. J.; Röhm, K.-H.; Kolbe, L. Inhibition of human tyrosinase requires molecular motifs distinctively different from mushroom tyrosinase. *J. Invest. Dermatol.* **2018**, *138*, 1601−1608.

(47) Mann, T.; Scherner, C.; Röhm, K.-H.; Kolbe, L. Structure-activity relationships of thiazolyl resorcinols, potent and selective inhibitors of human tyrosinase. *Int. J. Mol. Sci.* **2018**, *19*, 690.

(48) Ismaya, W. T.; Rozeboom, H. J.; Weijn, A.; Mes, J. J.; Fusetti, F.; Wichers, H. J.; Dijkstra, B. W. Crystal structure of *Agaricus bisporus* mushroom tyrosinase: identity of the tetramer subunits and interaction with tropolone. *Biochemistry* **2011**, *50*, 5477−5486.

(49) P14679 *Homo sapiens* Tyrosinase Model. https://swissmodel.expasy.org/repository/uniprot/P14679 (accessed Jul 17, 2020).

(50) Lai, X.; Wichers, H. J.; Soler-Lopez, M.; Dijkstra, B. W. Structure of human tyrosinase related protein 1 reveals a binuclear zinc active site important for melanogenesis. *Angew. Chem., Int. Ed.* **2017**, *56*, 9812−9815.

(51) Pretzler, M.; Bijelic, A.; Rompel, A. Heterologous expression and characterization of functional mushroom tyrosinase (*Ab*PPO4). *Sci. Rep.* **2017**, *7*, 1810.

(52) Lai, X.; Wichers, H. J.; Soler-Lopez, M.; Dijkstra, B. W. Structure and function of human tyrosinase and tyrosinase-related proteins. *Chem. - Eur. J.* **2018**, *24*, 47−55.

(53) Spritz, R. A.; Oh, J.; Fukai, K.; Holmes, S. A.; Ho, L.; Chitayat, D.; France, T. D.; Musarella, M. A.; Orlow, S. J.; Schnur, R. E.; Weleber, R. G.; Levin, A. V. Novel mutations of the tyrosinase (*TYR*) gene in type I oculocutaneous albinism (OCA1). *Hum. Mutat.* **1997**, *10*, 171−174.

(54) Peyroux, E.; Ghattas, W.; Hardré, R.; Giorgi, M.; Faure, B.; Simaan, A. J.; Belle, C.; Réglier, M. Binding of 2-hydroxypyridine-*N*-oxide on dicopper(II) centers: insights into tyrosinase inhibition mechanism by transition-state analogs. *Inorg. Chem.* **2009**, *48*, 10874−10876.

(55) Kolbe, L.; Mann, T.; Gerwat, W.; Batzer, J.; Ahlheit, S.; Scherner, C.; Wenck, H.; Stäb, F. 4-n-butylresorcinol, a highly effective tyrosinase inhibitor for the topical treatment of hyperpigmentation. *J. Eur. Acad. Dermatol. Venereol.* **2013**, *27*, 19−23.

(56) Garcia-Jimenez, A.; Teruel-Puche, J. A.; Berna, J.; Rodriguez-Lopez, J. N.; Tudela, J.; Garcia-Ruiz, P. A.; Garcia-Canovas, F. Characterization of the action of tyrosinase on resorcinols. *Bioorg. Med. Chem.* **2016**, *24*, 4434−4443.

(57) Cordes, P.; Sun, W.; Wolber, R.; Kolbe, L.; Klebe, G.; Röhm, K.-H. Expression in non-melanogenic systems and purification of soluble variants of human tyrosinase. *Biol. Chem.* **2013**, *394*, 685−693.

(58) Nishioka, K. Particulate tyrosinase of human malignant melanoma. *Eur. J. Biochem.* **1978**, *85*, 137−146.

(59) Wood, J. M.; Schallreuter, K. U. Studies on the reactions between human tyrosinase, superoxide anion, hydrogen peroxide and thiols. *Biochim. Biophys. Acta, Gen. Subj.* **1991**, *1074*, 378−385.

(60) Kong, K.-H.; Park, S.-Y.; Hong, M.-P.; Cho, S.-H. Expression and characterization of human tyrosinase from a bacterial expression system. *Comp. Biochem. Physiol., Part B: Biochem. Mol. Biol.* **2000**, *125*, 563−569.

(61) Kong, J.-N.; Lee, H.-J.; Jo, D.-H.; Kong, K.-H. Characterization of human tyrosinase ectodomain expressed in *Escherichia coli*. *Protein Pept. Lett.* **2010**, *17*, 1026−1030.

(62) Dolinska, M. B.; Kovaleva, E.; Backlund, P.; Wingfield, P. T.; Brooks, B. P.; Sergeev, Y. V. Albinism-causing mutations in recombinant human tyrosinase alter intrinsic enzymatic activity. *PLoS One* **2014**, *9*, e84494.

(63) Dolinska, M. B.; Sergeev, Y. V. The consequences of deglycosylation of recombinant intra-melanosomal domain of human tyrosinase. *Biol. Chem.* **2017**, *399*, 73−77.

(64) Branza-Nichita, N.; Negroiu, G.; Petrescu, A. J.; Garman, E. F.; Platt, F. M.; Wormald, M. R.; Dwek, R. A.; Petrescu, S. M. Mutations at critical *N*-glycosylation sites reduce tyrosinase activity by altering folding and quality control. *J. Biol. Chem.* **2000**, *275*, 8169−8175.

(65) Kus, N. J.; Dolinska, M. B.; Young, K. L.; Dimitriadis, E. K.; Wingfield, P. T.; Sergeev, Y. V. Membrane-associated human tyrosinase is an enzymatically active monomeric glycoprotein. *PLoS One* **2018**, *13*, e0198247.

(66) Favre, E.; Daina, A.; Carrupt, P.-A.; Nurisso, A. Modeling the met form of human tyrosinase: a refined and hydrated pocket for antagonist design. *Chem. Biol. Drug Des.* **2014**, *84*, 206−215.

(67) Yang, F.; Boissy, R. E. Effects of 4-tertiary butylphenol on the tyrosinase activity in human melanocytes. *Pigm. Cell Res.* **1999**, *12*, 237−245.

(68) Yamazaki, Y.; Kawano, Y. *N*-(3,5-Dihydroxybenzoyl)-6-hydroxytryptamine as a novel human tyrosinase inhibitor that inactivates the enzyme in cooperation with L-3,4-dihydroxyphenylalanine. *Chem. Pharm. Bull.* **2010**, *58*, 1536−1540.

(69) Song, K.; An, S. M.; Kim, M.; Koh, J.-S.; Boo, Y. C. Comparison of the antimelanogenic effects of *p*-coumaric acid and its methyl ester and their skin permeabilities. *J. Dermatol. Sci.* **2011**, *63*, 17−22.

(70) Kwak, J. Y.; Park, S.; Seok, J. K.; Liu, K.-H.; Boo, Y. C. Ascorbyl coumarates as multifunctional cosmeceutical agents that inhibit melanogenesis and enhance collagen synthesis. *Arch. Dermatol. Res.* **2015**, *307*, 635−643.

(71) Micillo, R.; Sires-Campos, J.; Garcia-Borron, J. C.; Panzella, L.; Napolitano, A.; Olivares, C. Conjugation with dihydrolipoic acid imparts caffeic acid ester potent inhibitory effect on dopa oxidase activity of human tyrosinase. *Int. J. Mol. Sci.* **2018**, *19*, 2156.

(72) Kim, M.; Park, J.; Song, K.; Kim, H. G.; Koh, J.-S.; Boo, Y. C. Screening of plant extracts for human tyrosinase inhibiting effects. *Int. J. Cosmet. Sci.* **2012**, *34*, 202−208.

(73) Park, J.; Boo, Y. C. Isolation of resveratrol from *Vitis viniferae* caulis and its potent inhibition of human tyrosinase. *Evidence-Based Complementary Altern. Med.* **2013**, *2013*, 645257.

(74) An, S. M.; Koh, J.-S.; Boo, Y. C. *p*-Coumaric acid not only inhibits human tyrosinase activity *in vitro* but also melanogenesis in cells exposed to UVB. *Phytother. Res.* **2010**, *24*, 1175−1180.

(75) Park, J.; Park, J. H.; Suh, H.-J.; Lee, I. C.; Koh, J.; Boo, Y. C. Effects of resveratrol, oxyresveratrol, and their acetylated derivatives on cellular melanogenesis. *Arch. Dermatol. Res.* **2014**, *306*, 475−487.

(76) Park, S.; Seok, J. K.; Kwak, J. Y.; Choi, Y.-H.; Hong, S. S.; Suh, H.-J.; Park, W.; Boo, Y. C. Anti-melanogenic effects of resveratryl triglycolate, a novel hybrid compound derived by esterification of resveratrol with glycolic acid. *Arch. Dermatol. Res.* **2016**, *308*, 325−334.

(77) Kwak, J. Y.; Seok, J. K.; Suh, H.-J.; Choi, Y.-H.; Hong, S. S.; Kim, D. S.; Boo, Y. C. Antimelanogenic effects of luteolin 7-sulfate isolated from *Phyllospadix iwatensis* Makino. *Br. J. Dermatol.* **2016**, *175*, 501−511.

(78) Lin, Y.-P.; Hsu, F.-L.; Chen, C.-S.; Chern, J.-W.; Lee, M.-H. Constituents from the Formosan apple reduce tyrosinase activity in human epidermal melanocytes. *Phytochemistry* **2007**, *68*, 1189−1199.

(79) Okombi, S.; Rival, D.; Bonnet, S.; Mariotte, A.-M.; Perrier, E.; Boumendjel, A. Discovery of benzylidenebenzofuran-3(2*H*)-one (aurones) as inhibitors of tyrosinase derived from human melanocytes. *J. Med. Chem.* **2006**, *49*, 329−333.

(80) Leoty-Okombi, S.; Bonnet, S.; Rival, D.; Degrave, V.; Lin, X.; Vogelgesang, B.; André-Frei, V. In vitro melanogenesis inhibitory effects of *N*-feruloyldopamine. *J. Cosmet. Sci.* **2013**, *64*, 133−144.

(81) Wang, H.-M.; Chen, C.-Y.; Wen, Z.-H. Identifying melanogenesis inhibitors from *Cinnamomum subavenium* with *in vitro* and *in vivo* screening systems by targeting the human tyrosinase. *Exp. Dermatol.* **2011**, *20*, 242−248.

(82) Lo, Y.-H.; Lin, R.-D.; Lin, Y.-P.; Liu, Y.-L.; Lee, M.-H. Active constituents from *Sophora japonica* exhibiting cellular tyrosinase inhibition in human epidermal melanocytes. *J. Ethnopharmacol.* **2009**, *124*, 625−629.

(83) Tu, C.-X.; Lin, M.; Lu, S.-S.; Qi, X.-Y.; Zhang, R.-X.; Zhang, Y.-Y. Curcumin inhibits melanogenesis in human melanocytes. *Phytother. Res.* **2012**, *26*, 174−179.

(84) Kanehira, T.; Takekoshi, S.; Nagata, H.; Osamura, R. Y.; Homma, T. Kinobeon A as a potent tyrosinase inhibitor from cell culture of safflower: *in vitro* comparisons of kinobeon A with other putative inhibitors. *Planta Med.* **2003**, *69*, 457−459.

(85) Bradley, S. E.; Collington, E. W.; Fyfe, M. C. T.; Gattrell, W. T.; Geden, J. V.; Murray, P. J.; Procter, M. J.; Rowley, R. J.; Williams, J. G. Resorcinol Derivatives. PCT WO02/24613, 2002.

(86) Gonzalvez, A.; Gonzalez Ureña, A. G.; Lewis, R. J.; van der Zwan, G. Spectroscopy and kinetics of tyrosinase catalyzed *trans*-resveratrol oxidation. *J. Phys. Chem. B* **2012**, *116*, 2553−2560.

(87) Haghbeen, K.; Tan, E. W. Direct spectrophotometric assay of monooxygenase and oxidase activities of mushroom tyrosinase in the presence of synthetic and natural substrates. *Anal. Biochem.* **2003**, *312*, 23−32.

(88) Dubois, C.; Haudecoeur, R.; Orio, M.; Belle, C.; Bochot, C.; Boumendjel, A.; Hardré, R.; Jamet, H.; Réglier, M. Versatile effect of aurone structure on mushroom tyrosinase activity. *ChemBioChem* **2012**, *13*, 559−565.

(89) Haudecoeur, R.; Gouron, A.; Dubois, C.; Jamet, H.; Lightbody, M.; Hardré, R.; Milet, A.; Bergantino, E.; Bubacco, L.; Belle, C.; Réglier, M.; Boumendjel, A. Investigation of binding-site homology between mushroom and bacterial tyrosinases by using aurones as effectors. *ChemBioChem* **2014**, *15*, 1325−1333.

(90) Markova, E.; Kotik, M.; Krenkova, A.; Man, P.; Haudecoeur, R.; Boumendjel, A.; Hardré, R.; Mekmouche, Y.; Courvoisier-Dezord, E.; Réglier, M.; Martinkova, L. Recombinant tyrosinase from *Polyporus arcularius*: overproduction in *Escherichia coli*, characterization, and use in a study of aurones as tyrosinase effectors. *J. Agric. Food Chem.* **2016**, *64*, 2925−2931.

(91) Balyan, R.; Kudugunti, S. K.; Hamad, H. A.; Yousef, M. S.; Moridani, M. Y. Bioactivation of luteolin by tyrosinase selectively

inhibits glutathione S-transferase. *Chem.-Biol. Interact.* **2015**, *240*, 208−218.

(92) Yoshimori, A.; Oyama, T.; Takahashi, S.; Abe, H.; Kamiya, T.; Abe, T.; Tanuma, S. Structure-activity relationships of the thujaplicins for inhibition of human tyrosinase. *Bioorg. Med. Chem.* **2014**, *22*, 6193−6200.

(93) Mädel, A. Strukturbasierte Entwicklung von Inhibitoren der humanen Tyrosinase und der Farnesyltransferase. Ph.D. Thesis, Philipps-Universität Marburg, 2009.

(94) Schlich, M.; Fornasier, M.; Nieddu, M.; Sinico, C.; Murgia, S.; Rescigno, A. 3-Hydroxycoumarin loaded vesicles for recombinant human tyrosinase inhibition in topical applications. *Colloids Surf., B* **2018**, *171*, 675−681.

(95) Desmedt, B.; Courselle, P.; De Beer, J. O.; Rogiers, V.; Grosber, M.; Deconinck, E.; De Paepe, K. Overview of skin whitening agents with an insight into the illegal cosmetic market in Europe. *J. Eur. Acad. Dermatol. Venereol.* **2016**, *30*, 943−950.

(96) Khemis, A.; Kaiafa, A.; Queille-Roussel, C.; Duteil, L.; Ortonne, J.-P. Evaluation of efficacy and safety of rucinol serum in patients with melasma: a randomized controlled trial. *Br. J. Dermatol.* **2007**, *156*, 997−1004.

(97) Huh, S. Y.; Shin, J.-W.; Na, J.-I.; Huh, C.-H.; Youn, S.-W.; Park, K.-C. Efficacy and safety of liposome-encapsulated 4-*n*-butylresorcinol 0.1% cream for the treatment of melasma: A randomized controlled split-face trial. *J. Dermatol.* **2010**, *37*, 311−315.

(98) Arrowitz, C.; Schoelermann, A. M.; Mann, T.; Jiang, L. I.; Weber, T.; Kolbe, L. Effective tyrosinase inhibition by thiamidol results in significant improvement of mild to moderate melasma. *J. Invest. Dermatol.* **2019**, *139*, 1691−1698.

(99) Philipp-Dormston, W. G.; Vila Echagüe, A.; Pérez Damonte, S. H.; Riedel, J.; Filbry, A.; Warnke, K.; Lofrano, C.; Roggenkamp, D.; Nippel, G. Thiamidol containing treatment regimens in facial hyperpigmentation: An international multi-center approach consisting of a double-blind, controlled, split-face study and of an open label, real-world study. *Int. J. Cosmet. Sci.* **2020**, *42*, 377−387.

(100) Institute of Dermatology (Thailand) and Beiersdorf. Efficacy and Tolerability of an Isobutylamido-thiazolyl-resorcinol Cream 0.2% for Facial Hyperpigmentation (NCT03926845). https://clinicaltrials.gov/ct2/show/NCT03926845 (accessed Jul 23, 2020).